1971

An investigation of subsequent yield phenomena

Joseph George Hoeg

Department: Mechanical and Aerospace Engineering

AN INVESTIGATION OF SUBSEQUENT YIELD PHENOMENA

BY

JOSEPH GEORGE HOEG, 1943-

A DISSERTATION

Presented to the Faculty of the Graduate School of the

UNIVERSITY OF MISSOURI - ROLLA

in Partial Fulfillment of the Requirements for the Degree

DOCTOR OF PHILOSOPHY

in

MECHANICAL ENGINEERING

1971

Robert L. Davis
Advisor

R.D. Roche

Jerry F. Lehnhoff

R.B. Oetting

S.J. Bagano

T.R. Fawcett RES

ABSTRACT

A method utilizing high pressure fluid environments is described whereby a three-dimensional subsequent yield surface was determined for 304 stainless steel. Cylindrical parent specimens of this material were prestrained in axial compression under fluid pressure and then small sub-specimens were sectioned from these parent specimens. Finite element techniques were used to optimize the parent specimen size so that a zone of uniform axial stress would result during the prestraining. Longitudinal strains in this zone were monitored during the prestraining and the sub-specimens were cut from this region in a manner that did not allow the machining to appreciably affect the properties of the specimens. Following this, conventional tension and compression tests were performed on the sub-specimens in various fluid pressure environments to determine the yield strengths for the prestrained material in the directions of the principal axis of prestrain and the two transverse axes. These data are used to construct the subsequent yield surface.

PREFACE

This report contains the results of research conducted in partial fulfillment of the requirements for the degree Doctor of Philosophy in Mechanical Engineering. The work was done in the Department of Mechanical Engineering at the University of Missouri-Rolla, under the direction of Dr. Robert Lane Davis of the Department of Engineering Mechanics.

The author would like to take this opportunity to thank the individuals and organizations who made this work possible. Among these are the Carpenter Technology Corporation, which provided the specimen material and the maraging steel required for some of the hardware, and the United States Bureau of Mines, which made heat treatment facilities available. The individuals who contributed to the conduct of this project are numerous and it is not possible to acknowledge each contribution in the confines of this preface. However, the assistance of Mr. F. Wilson Sherrill must not go without mention. The enthusiastic, sustained support of Mr. Sherrill was monumental.

Finally, the author wishes to extend great appreciation to Dr. Davis for his support and encouragement.

TABLE OF CONTENTS

LIST OF ILLUSTRATIONS

Figures Page

I. INTRODUCTION

A yield criterion specifies a state of stress which, when reached, will result in plastic flow in a material. When a virgin material is subjected to loads that impose only one stress component, the formulation of a yield criterion is straight forward. The problem becomes more complicated, however, when such a material sustains a more complex state of stress. In this case, parameters must be selected to predict yielding and the effect of each stress component on these parameters must be evaluated. Many such criteria have been formulated to predict yielding in virgin materials subjected to triaxial stresses. For example, in the von Mises yield condition, the second deviatoric stress invariant is chosen as the governing parameter and, as a consequence, the hydrostatic stress component is assumed to be insignificant in determining whether or not yielding has occurred. Similarly, the Tresca yield condition assumes that the intermediate principal stress has no effect on yielding since the Tresca theory considers the maximum shearing stress as the parameter governing yielding.

All of these yield criteria can be categorized as either including, or not including, the effects of hydrostatic stresses. Currently, only yield conditions that neglect the effects of hydrostatic stresses enjoy widespread use. Experimental data has shown that early conclusions, which state that the effect of hydrostatic stresses on plastic flow is insignificant, are in error. As a result,

many researchers have proposed that the hydrostatic stress component be included in a yield criterion. The effect of the hydrostatic stress component on yielding in virgin materials is dependent upon the material under consideration and, indeed, this effect can be significant. Further, this effect can be of even greater significance when yielding in a prestrained, non-virgin, material is under study - an idea to be brought out in greater detail in the literature survey.

The reason for studying yielding in prestrained materials is that most load carrying members are non-virgin. Frequently, structural members are plastically deformed during the forming process. Prior plastic straining can also be the result of service use. One example of this is the intentional over-pressurization of thick-walled pressure vessels. The importance of subsequent yield theories transcends a multitude of engineering areas which involve stress reversals - wave propagation, metal forming, thermal stresses, etc. If, for example, a drawn pipe is loaded axially to stress levels below the conventionally defined yield point, yielding may go undetected if the non-isotropic characteristics generated by the drawing process are not fully recognized. Simultaneous application of torsional loads to this pipe will complicate the problem even further since the principal stress axes will now shift. Problems involving subsequent yielding will also occur in cyclically loaded members which are initially virgin if the stress

cycling is such that the yield strength for the virgin material is exceeded. To be able to consider these effects in general, one must understand the yielding process as it is described by conventionally accepted theories and by empirical data. The literature survey section of this paper discusses yield theories which attempt to account for previous material yielding. Despite the increasing sophistication appearing in more recent theories, theory is not yet in line with experimental data.

Because of the widespread application that would be available to a subsequent yield criterion, and because of the scarcity of documented information concerning such a criterion, the author has undertaken a research project aimed at the development of a yield model that will accommodate some of the more complicated effects associated with prestraining a material.

II. REVIEW OF LITERATURE

The two most frequently used yield theories - those of von Mises and Tresca - assume that the result of plastic straining is an isotropic expansion of the yield surface. The initial and subsequent yield surfaces as predicted by the von Mises criteria are shown in figure 1. The utility of the assumption of isotropic expansion lies in mathematical tractability rather than inherent accuracy. A simple compression test of a specimen prestrained plastically in tension might show that the yield surface does not always expand in an isotropic manner. A compressive yield strength somewhat lower than that for the virgin material could be observed. According to Dieter[1], this effect, known as the Bauschinger effect, results from the direction reversal of migrating dislocations. These dislocations "plow a path" in the microstructure during plastic straining, and they encounter a much lower resistance to migration when the direction of loading is reversed.

On a continuum scale, the manifestations of the Bauschinger effect are not at all well-behaved. Bridgman[2] found that some materials could be prestrained to a point where the Bauschinger effect is no longer evident. Still other materials do not even exhibit the effect at all. At this point, the most important thing is to realize that the Bauschinger effect is one of the oddities associated with plastic flow in some materials and a yield criteria must be able to accommodate it.

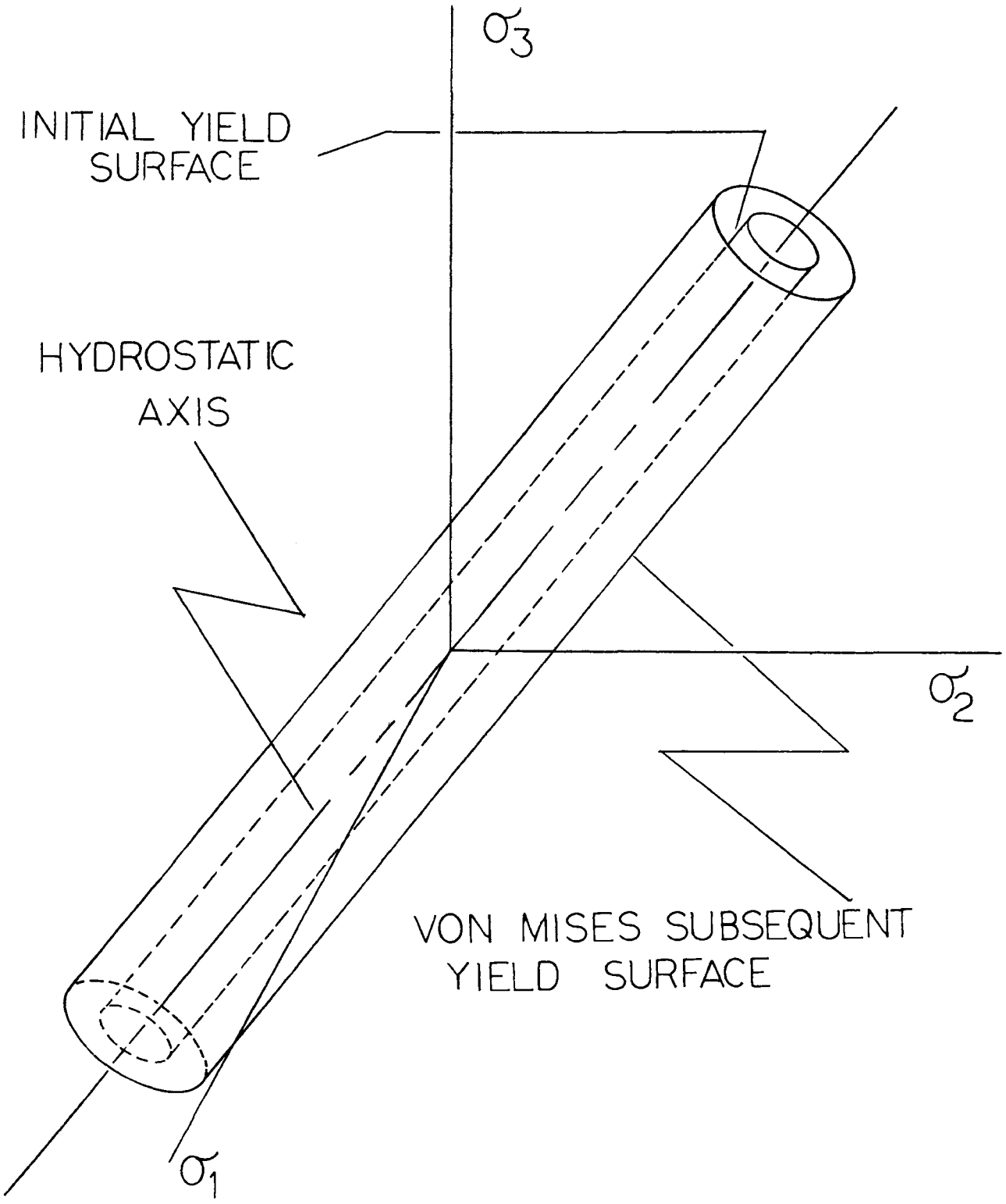

Figure 1 - Von Mises Initial and Subsequent yield Surfaces

Prager[3] has devised a kinematic hardening model which describes the subsequent yielding phenomenon in terms which can be applied to continuum mechanics formulations, but this model also has its shortcomings. When applied to two- or three-dimensional loadings, the inability of the yield locus or yield surface to change shape as it is being displaced puts the model in conflict with experimental data. The Prager model for uniaxial loading is shown in figure 2. These diagrams simply illustrate the hypothesis that a material has a fixed elastic unloading range. The movement of point P to the right represents a straining in a particular direction. As long as P does not touch the end of the linkage slot (as in figure 2c), the straining is elastic. If, after the point P has contacted the end of the linkage slot, the straining is continued, the linkage will be pulled to the right which is representative of plastic straining. Since the linkage has now been displaced to the right, the left end of the slot is now closer to the "no-load" position than it was originally (as in figure 2f). This symbolizes a reduction in yield strength as the loading direction is reversed.

The two-dimensional kinematic model is shown in figure 3. In this case, the Tresca hexagon shifts instead of just a slotted link. The loading vector pushes the hexagon along a principal axis until the loading vector tip locks into a corner. At this point the hexagon begins to shift along a line parallel to the loading vector. In its most general

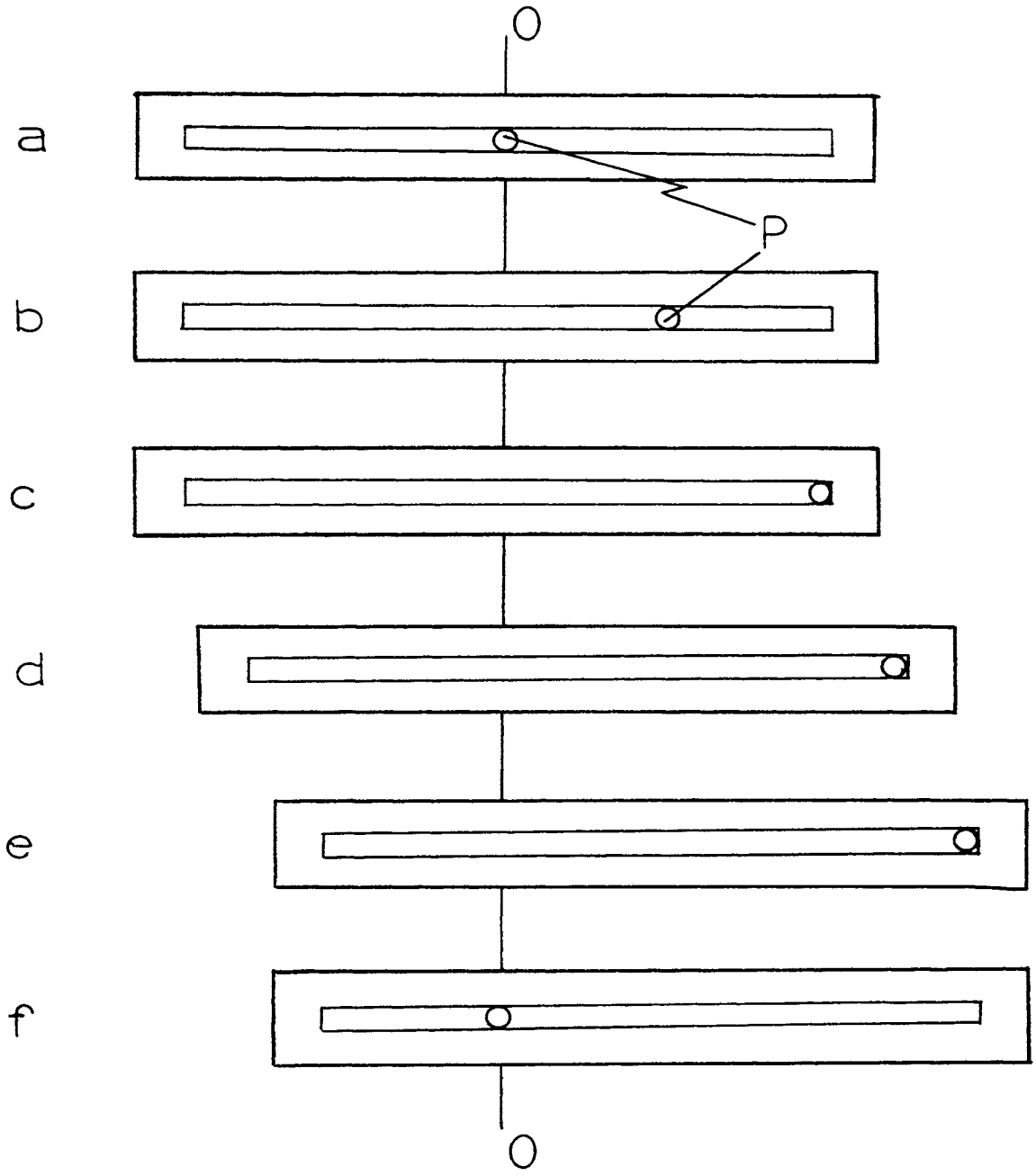

Figure 2 - Prager Kinematic Model for Uniaxial Loading

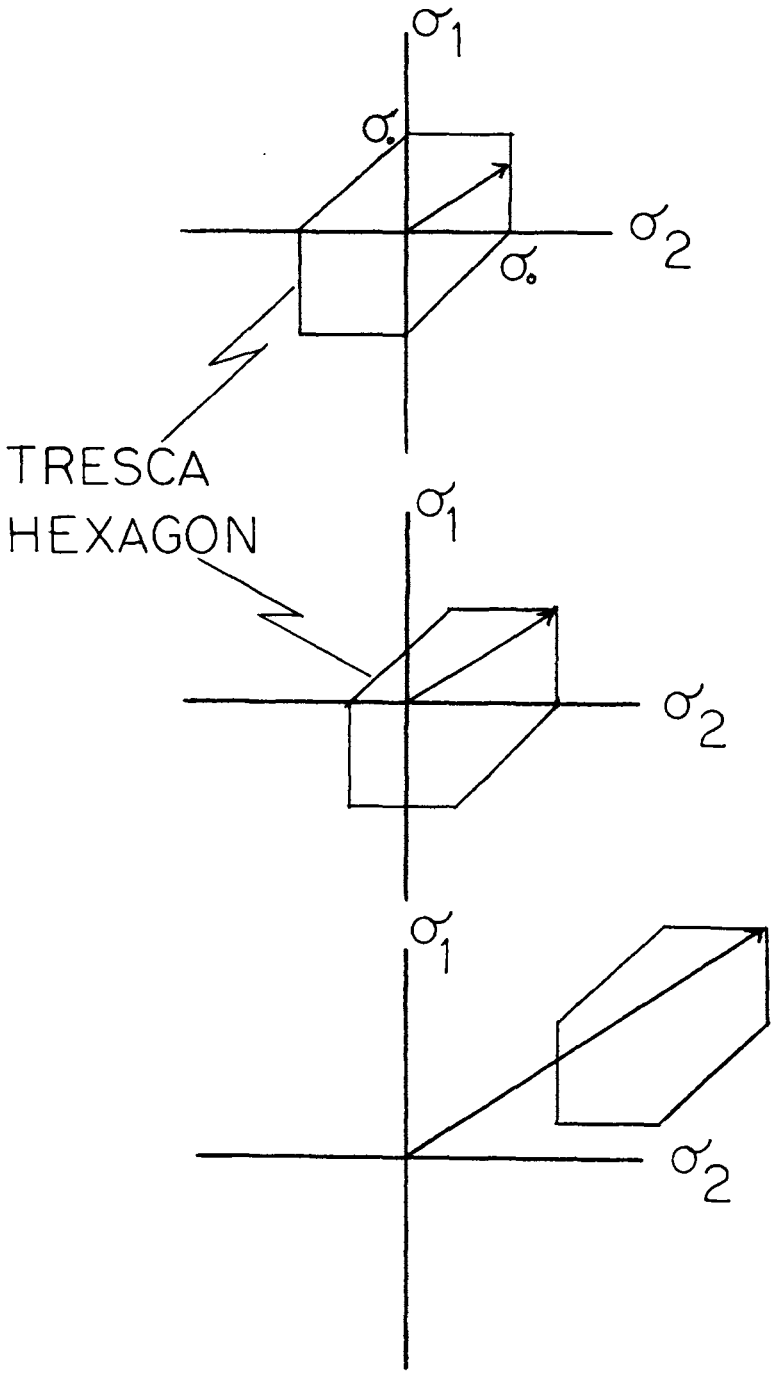

Figure 3 - Two-dimensional Kinematic Yield Model

form, the concept of kinematic hardening can be best visualized by observing the von Mises yield surface projection in the deviatoric plane. Kinematic hardening simply causes a shift in the yield locus without any distortion to the curve. A hypothetical example of such an effect is illustrated in figure 4.

A major departure from these two theories resulted from the work of Naghdi, Essenburg and Koff[4]. These researchers determined that the yield curve in a particular two-dimensional case does not displace but, instead, expands outward in the direction of loading with a consequent inward contraction of other areas of the curve. By pre-loading thin-walled aluminum tubes in torsion, followed by re-loading with various ratios of torsion and tension, they obtained the subsequent yield curves shown in figure 5. Unfortunately, it is difficult to express the type of data obtained by Naghdi et al in principal stress space. In cases such as torsion, where the principal stress axes do not remain fixed, it is necessary to know the amount of shift of the current principal stress axes with respect to some arbitrary stationary reference so that the stress vector at a point can be properly located in the stationary reference system.

Despite this drawback, tests involving the combined torsion and tension of thin-walled cylinders are widely used for work directed towards developing subsequent yield criteria. Minor variations of the Naghdi experiments have

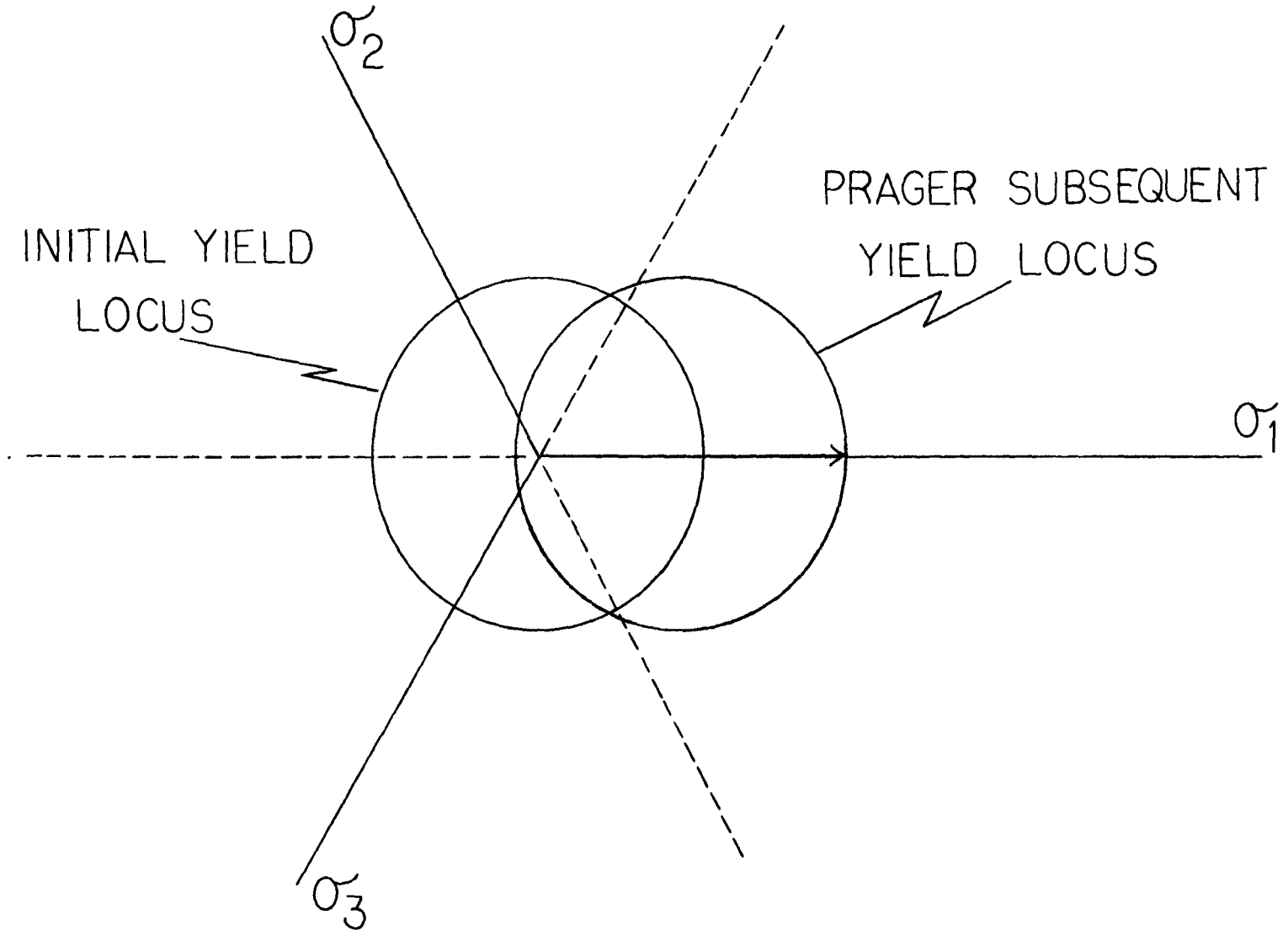

Figure 4 - Kinematic Yield Model in the Deviatoric Plane

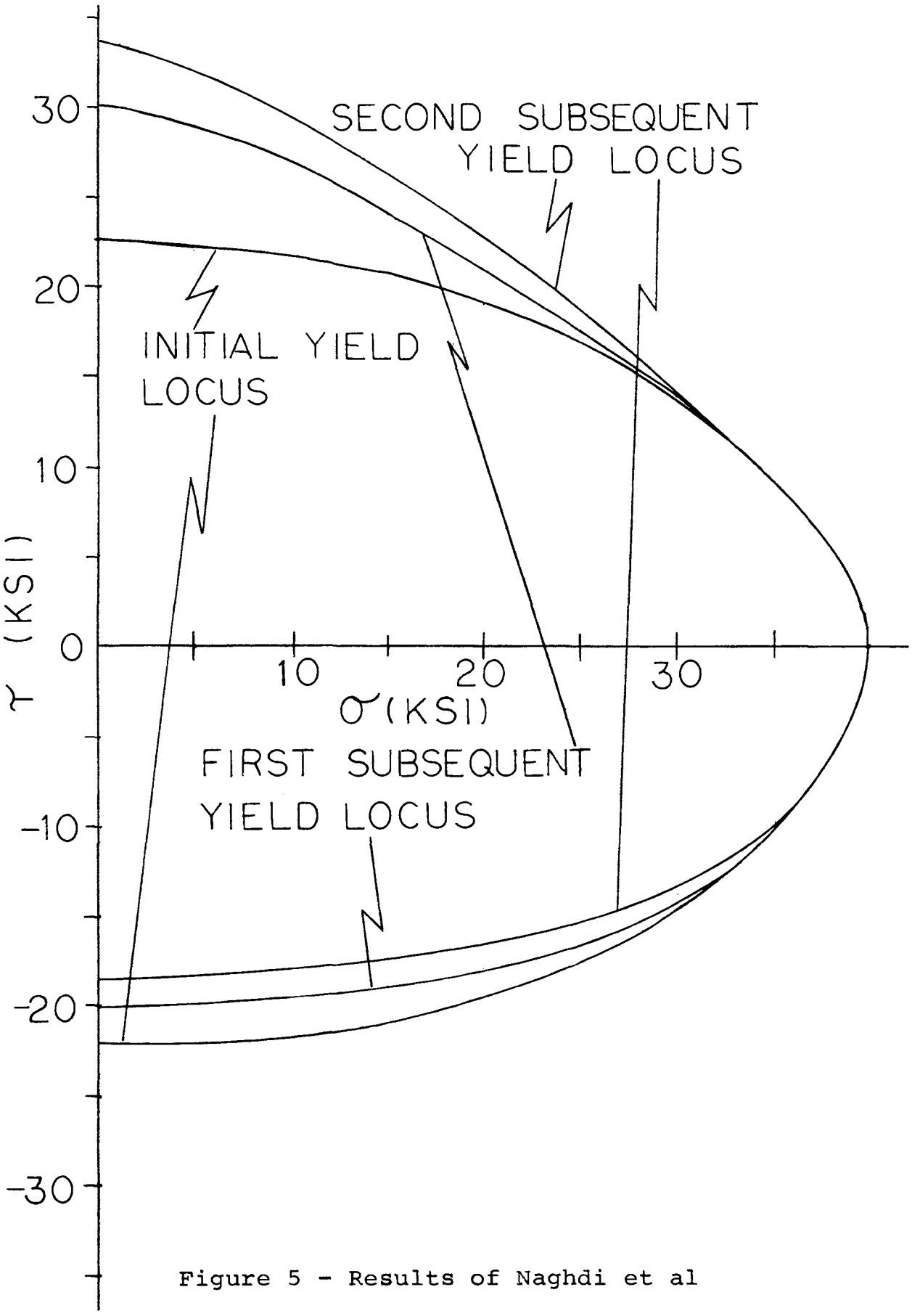

Figure 5 - Results of Naghdi et al

been performed on thin-walled tubes of aluminum, by Ivey[5] and Smith and Almroth[6]; copper, by Mair and Pugh[7]; and nickle, by Iagn and Shishmarev[8]. The data resulting from the tension-torsion tests of thin-walled cylinders are almost invariably presented in terms of a shear stress parameter and a normal stress parameter in a manner similar to that shown in figure 5. Despite the fact that this data presentation is not in principal stress coordinates, the presentation is still adequate enough to convey the idea that the observed phenomenon is neither purely isotropic nor purely kinematic in nature.

In an attempt to generalize the method of presentation of yield data for prestrained materials, Hsu[9] has developed a method which transforms data such as that of Naghdi et al into the deviatoric plane. The most significant problem with Hsu's method is that some of the torsion-tension data for thin-walled cylinders transform into yield loci, in the deviatoric plane, that show concavities. In addition, the method involves a method of describing local principal stress axis orientations that does not seem particularly well suited to handling states of stress which are more complex than those encountered in the experiments of Naghdi et al.

Thin-walled aluminum cylinders were also used by Hu and Bratt[10] in tests that involved axial tension and internal pressure. After axial prestraining, the specimens were subjected to combined axial tension and internal pressure

in order to determine the subsequent yield loci. These data are presented in principal stress coordinates in figure 6. By projecting the data in figure 6 along lines normal to the deviatoric plane, the deviatoric representation can be obtained and is shown in figure 7. Implicit in this projection technique is the pressure-independence of the yield strength of this material - an assumption that may be in error.

No information was published on three-dimensional subsequent yield surfaces until Hu[11] described a series of experiments in which the expansive deflections of yield surface elements were found to be a function of the proximity of a surface element to the loading vector tip. An example of a subsequent yield surface as proposed by Hu is shown in figure 8, and two sections of this surface lying normal to the hydrostatic axis are shown in figure 9. The author's literature survey has shown this to be the only published work connected with three-dimensional, subsequent yield surfaces and this statement is supported by a recent survey paper by Prager[12].

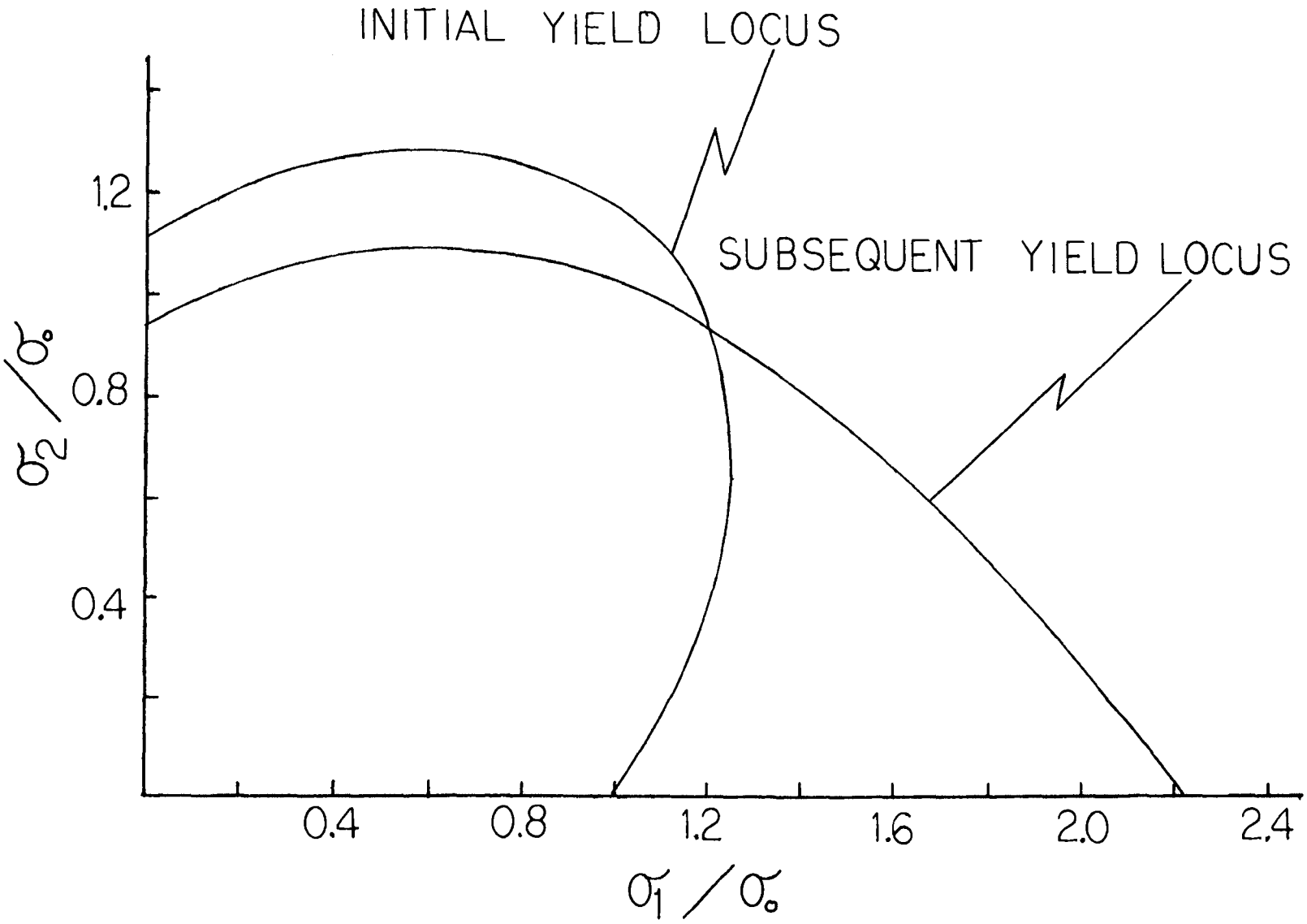

Figure 6 - Results of Hu and Bratt

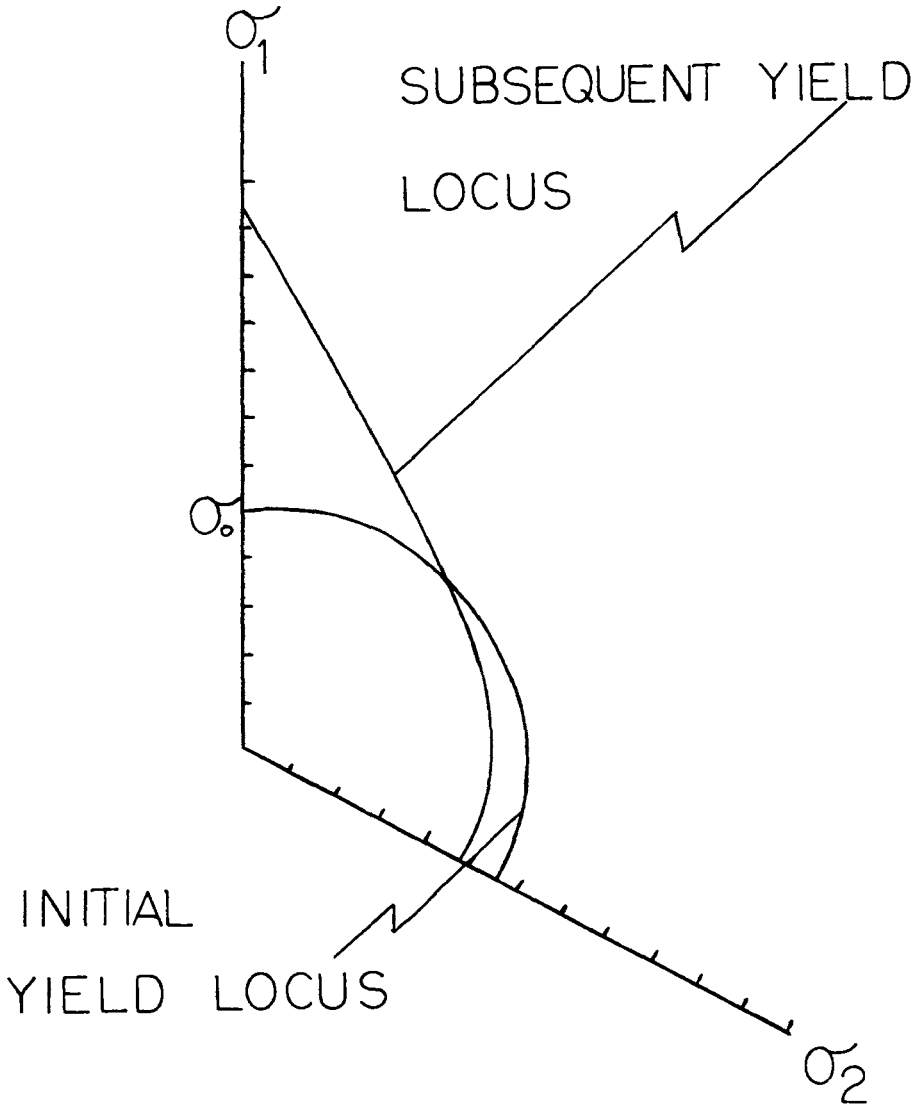

Figure 7 - Deviatoric Representation of the Results of Hu and Bratt

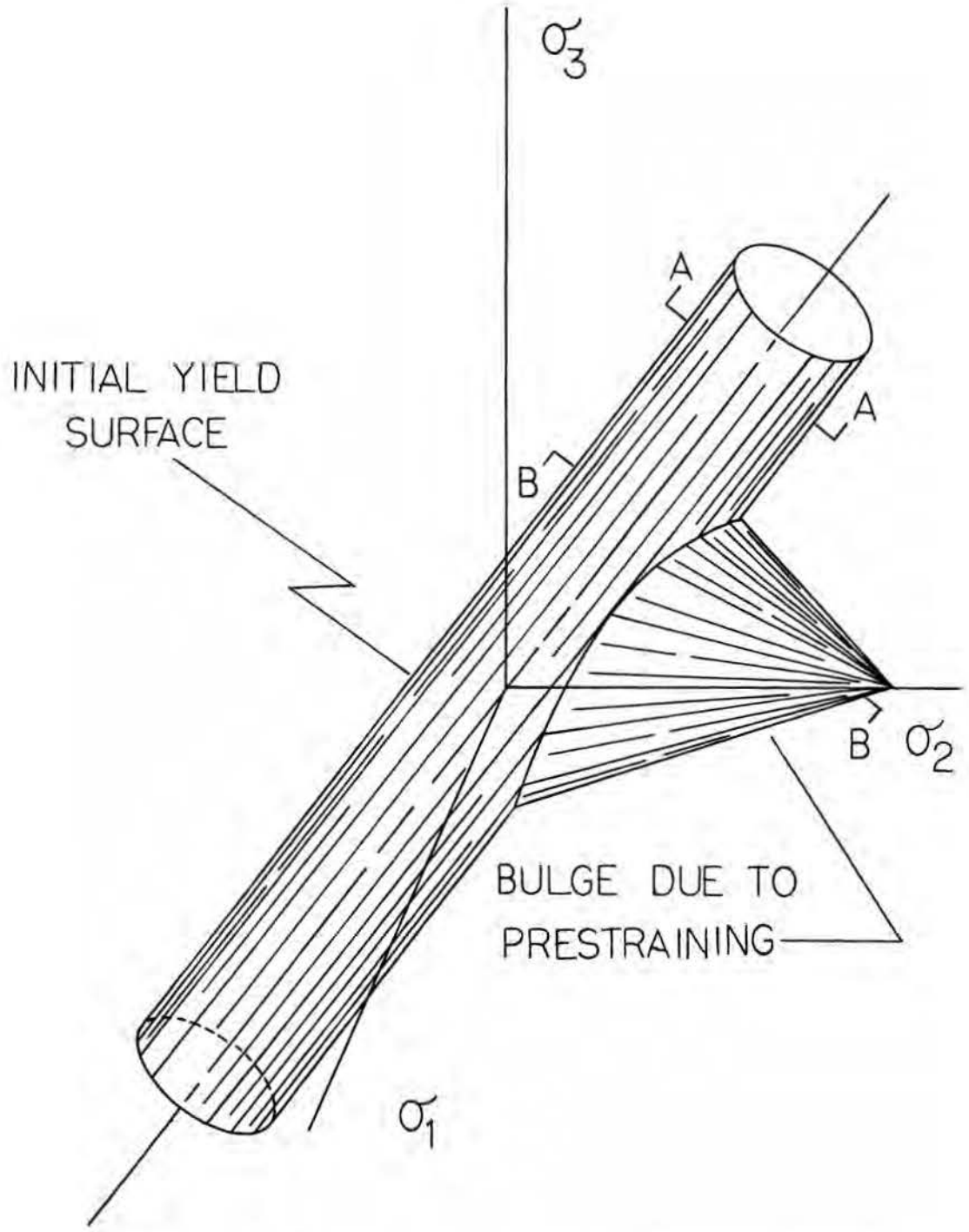

Figure 8 - Subsequent Yield Model Proposed by Hu

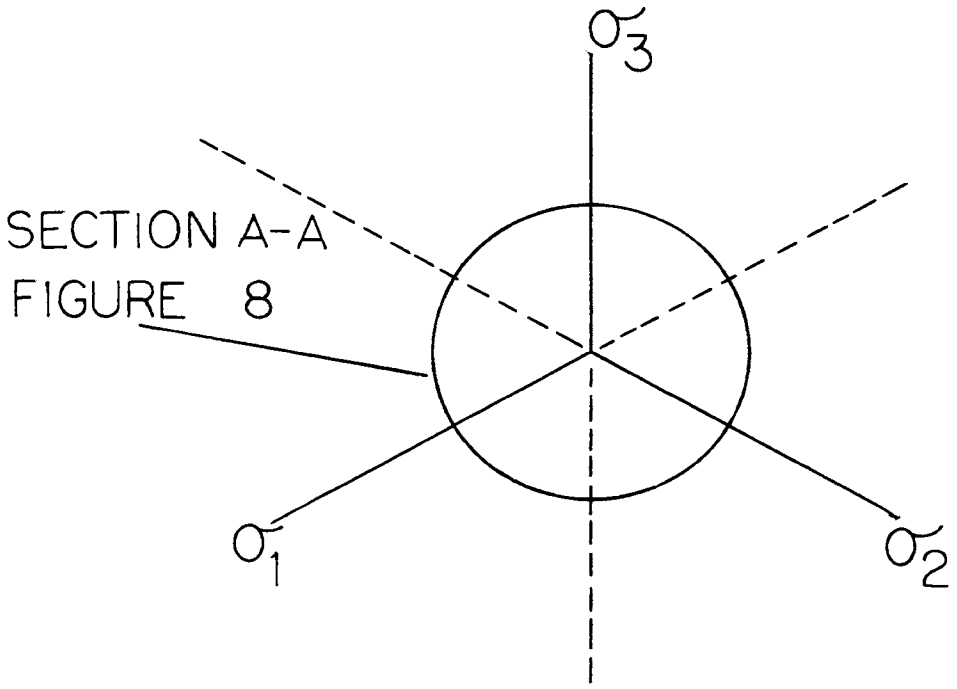

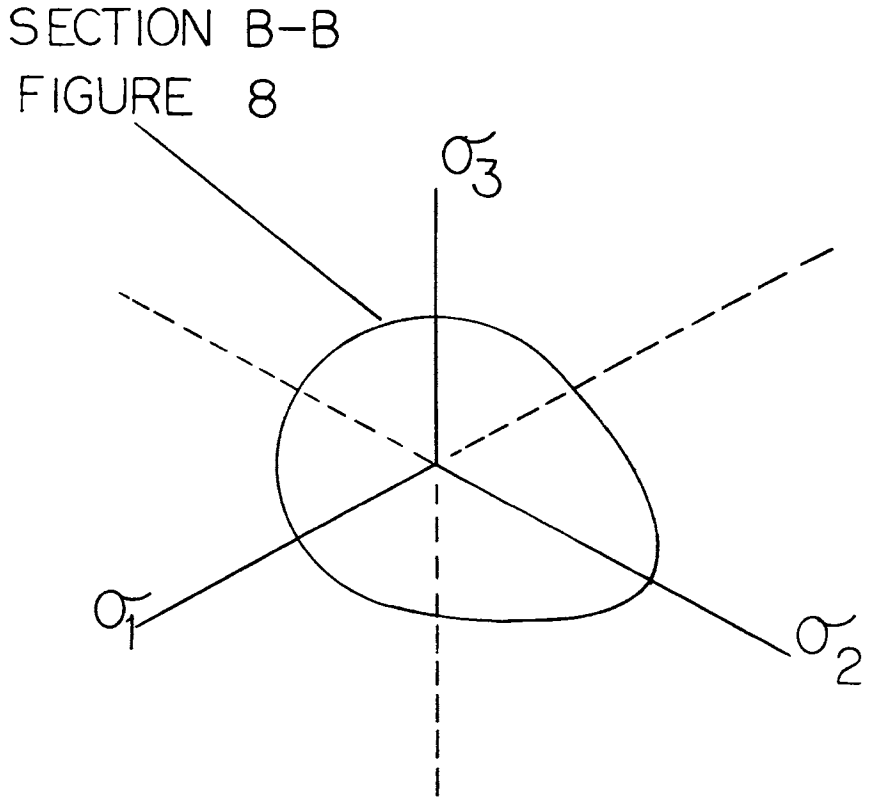

Figure 9 - Sections of the Hu Yield Model

III. DISCUSSION

A. Experimental Approach

Since most existing subsequent yield theories are in poor agreement with experimental data, an experimental effort which would generate a true subsequent yield surface seemed desirable. From this empirical surface a new subsequent yield theory could then be obtained. Most of the current subsequent yield data deals with two-dimensional stress states since this condition is relatively easy to produce in the laboratory. In order to develop a three-dimensional yield surface for a non-virgin material, conventional tension and compression tests of prestrained specimens can be conducted in a hydrostatic pressure environment. By varying the pressure environment from test to test, a significant portion of the yield surface then comes within experimental reach.

For reasons of economy of effort and material, compressive prestraining of a parent specimen that would yield several smaller sub-specimens was selected as the prestraining method for this program. The problem of prestraining a material, and then sectioning specimens from this for the tests to follow, involves several compromises. If the prestraining is done in an atmospheric environment, the loads can be applied in a conventional compression testing machine. Since high compressive loads are easily achieved, the cross-section of the parent specimen can be large which will allow, in turn, large

sub-specimens to be cut from a transverse axis. Opposing the obvious advantages of reasonably sized sub-specimens is the fact that the subsequent yield surface cannot be examined in detail below the point on the hydrostatic axis at which the prestraining was done, if this point is that of ambient pressure. Prestraining under a pressure environment will permit investigation of the subsequent yield surface below the pressure region of prestraining, but serious limitations are placed on the degree of prestrain to be achieved and the size of the parent specimens by the physical limitations of the environmental containment vessel and the pre-loading device. The second approach, i.e., prestraining under pressure, was chosen by the author since it is extremely desirable to investigate the subsequent yield surface at pressures above and below the pressure region where the prestraining was done. Also, the obstacles posed by the small size of the sub-specimens were not insurmountable. Ideally, the prestraining should be carried out under several different pressure environments. This would allow the influence of the prestraining environment on the subsequent yield surface to be studied. In order to provide at least fragmentary information in this area, a single parent specimen was prestrained in atmospheric pressure.

Consider, now, the π-plane (deviatoric plane) shown in figure 10. This is a view of an assumed von Mises yield surface for a virgin material as seen by looking down the

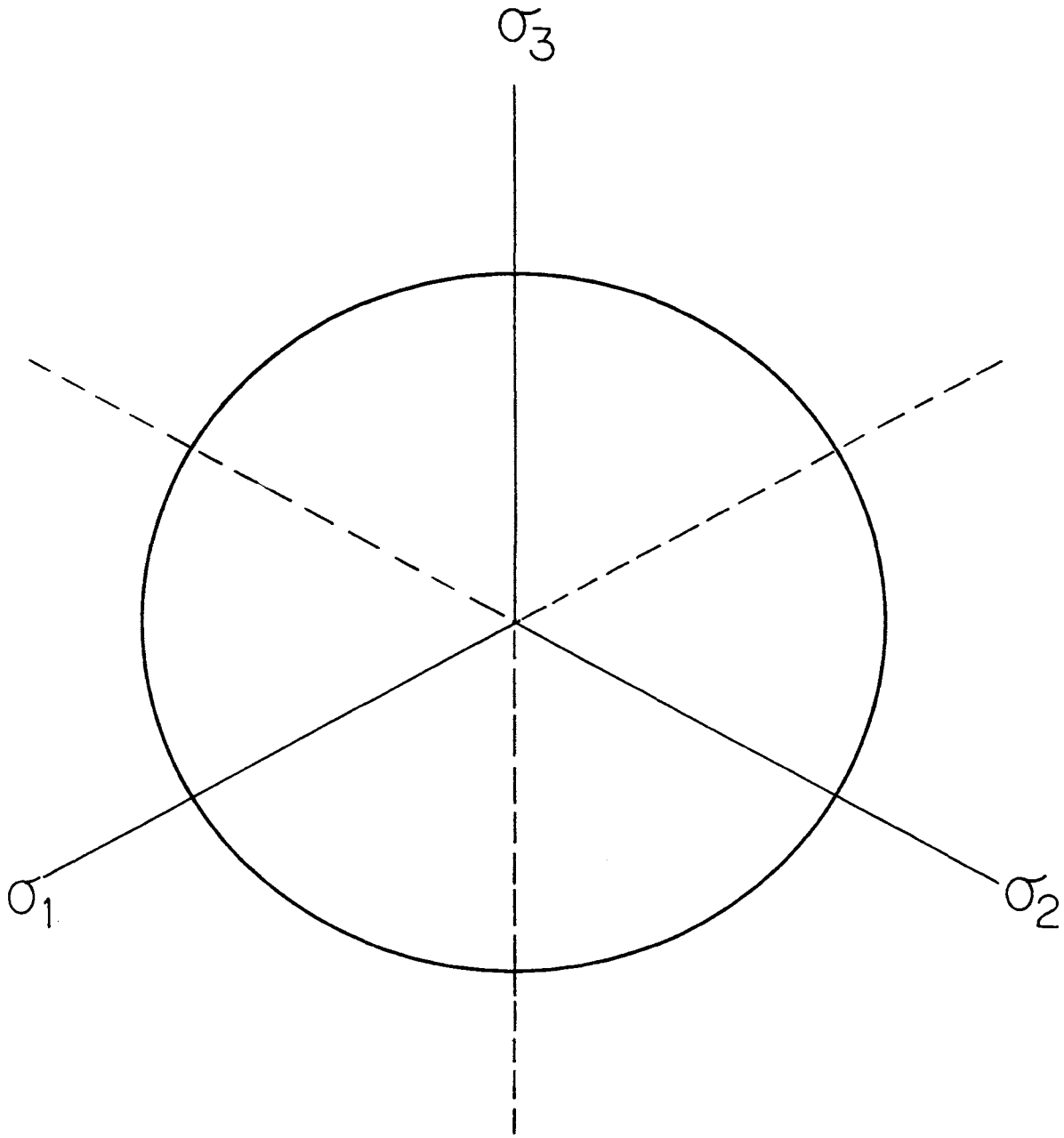

Figure 10 - Typical Yield Surface Projected in the Deviatoric Plane

hydrostatic axis. The projected principal axes and their extensions cut the circle into equal sectors. By assuming symmetry about a principal axis, say the axis of prestraining or σ_1, it is evident that at least four tests are required to sense the yield surface at a particular station along the hydrostatic axis. These tests are tension and compression along the direction of prestraining and tension and compression along an axis normal to the direction of prestraining. By performing this sequence of four tests in various pressure environments, sufficient data can be obtained to generate six lines which lie in the subsequent yield surface. This was the technique used in this project.

B. Selection of Material and Preparation of Specimens

Electing to do the parent specimen prestraining under a pressurized fluid environment presented several additional questions concerning parent specimen size, material selection and the environmental pressure level to be used for prestraining. Since the available fluid pressure generation facility was limited to 80,000 psi, it was decided to conduct the prestraining at half of that level - 40,000 psi. This would permit the subsequent yield surface to be investigated at environmental pressures ranging to levels of 40,000 psi above and below the prestraining pressure level.

Because of the size of the pressure chamber which was available (3" diameter by 11" length), a two inch diameter cylindrical compression slug was chosen for the parent specimen. This would permit transverse specimens of up to two inches in length to be sectioned from the slugs after prestraining. It was desirable to have the parent specimens as short as possible to avoid any buckling problems that might arise during plastic compressive prestraining, but it was also necessary to make them long enough so that a 2.5 inch long center portion would exist in which the axial stress distribution would be constant over the cross-section during the prestraining. In an elastic situation where the loads are applied as point loads, St. Venant's principal suggests that a 6.5-inch length would suffice. For this project, however, the

parent specimen would be squeezed between a lower support block and a movable upper platten, or adapter. The adapter fits on the end of a ram which protrudes through the pressure vessel and is used to distribute the pre-load over the parent specimen face. A schematic of this internal vessel set-up appears in figure 11.

In order to determine, with some certainty, an appropriate parent specimen length, a finite element stress analysis program was employed. At this point, the specimen was assumed to have a yield strength in compression of 35,000 psi and elastic and plastic moduli which conformed to those of 304 stainless steel. For purposes of comparison, this assumed stress-strain curve appears, with the 304 stainless steel curve, in figure 12. The point at which compressive straining was to cease was at a uniform axial stress of 60,000 psi. The required load was assumed to be evenly distributed over the ram-platten interface and the bottom of the support block was assumed to be axially constrained. The results of this analysis indicated that a 5.0 inch long parent specimen, subjected to an average compressive stress of 60,000 psi, would have a uniformly stressed center section 2.5 inches in length.

The problem of material selection was further complicated by the fact that the total prestraining load and pressure force on the ram could not exceed 300,000 lbs due to equipment limitations and, beyond this, by the fact that a ram of relatively small diameter had to carry this

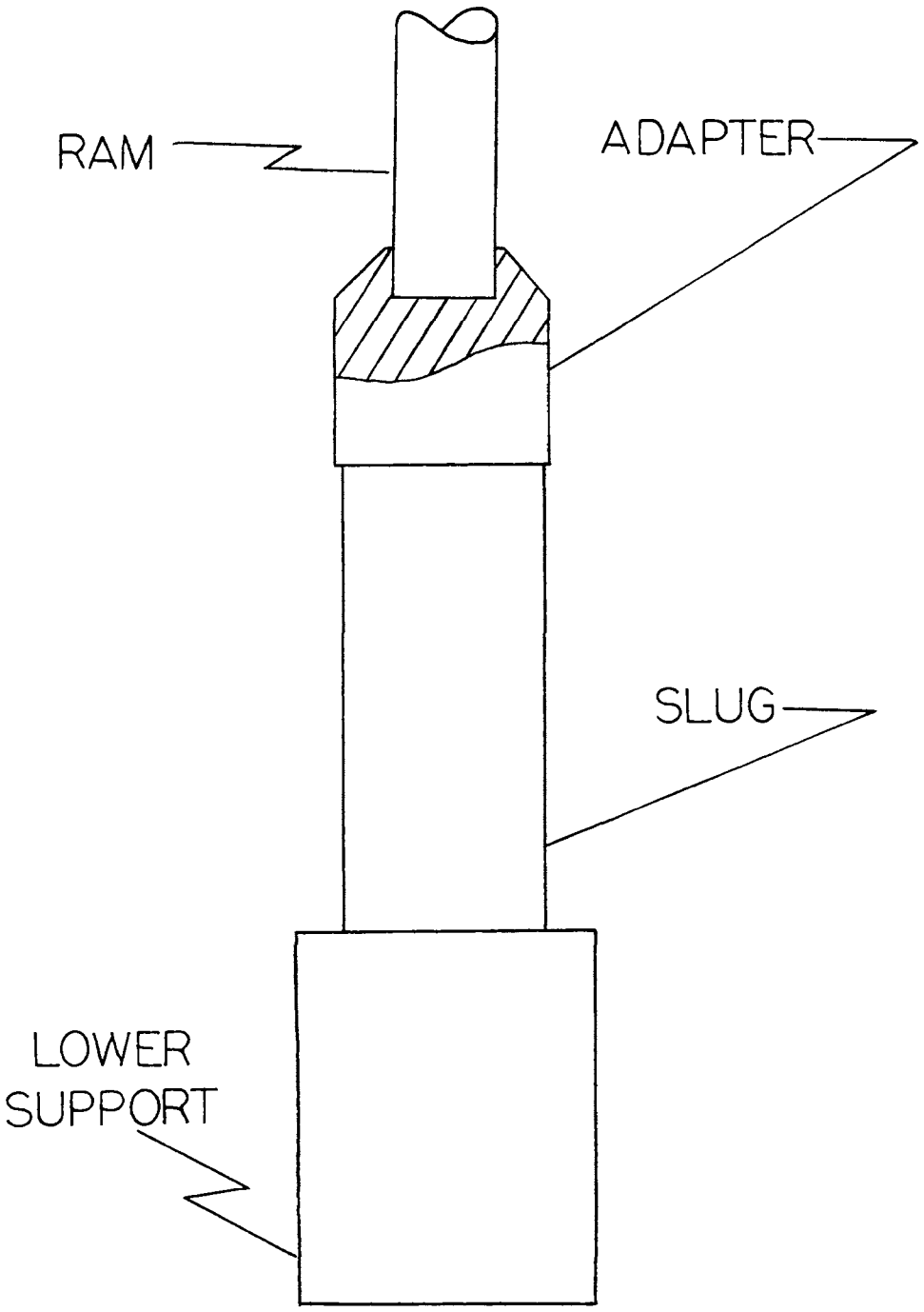

Figure 11 - Schematic of Internal Vessel Hardware used for Parent Specimen Prestraining

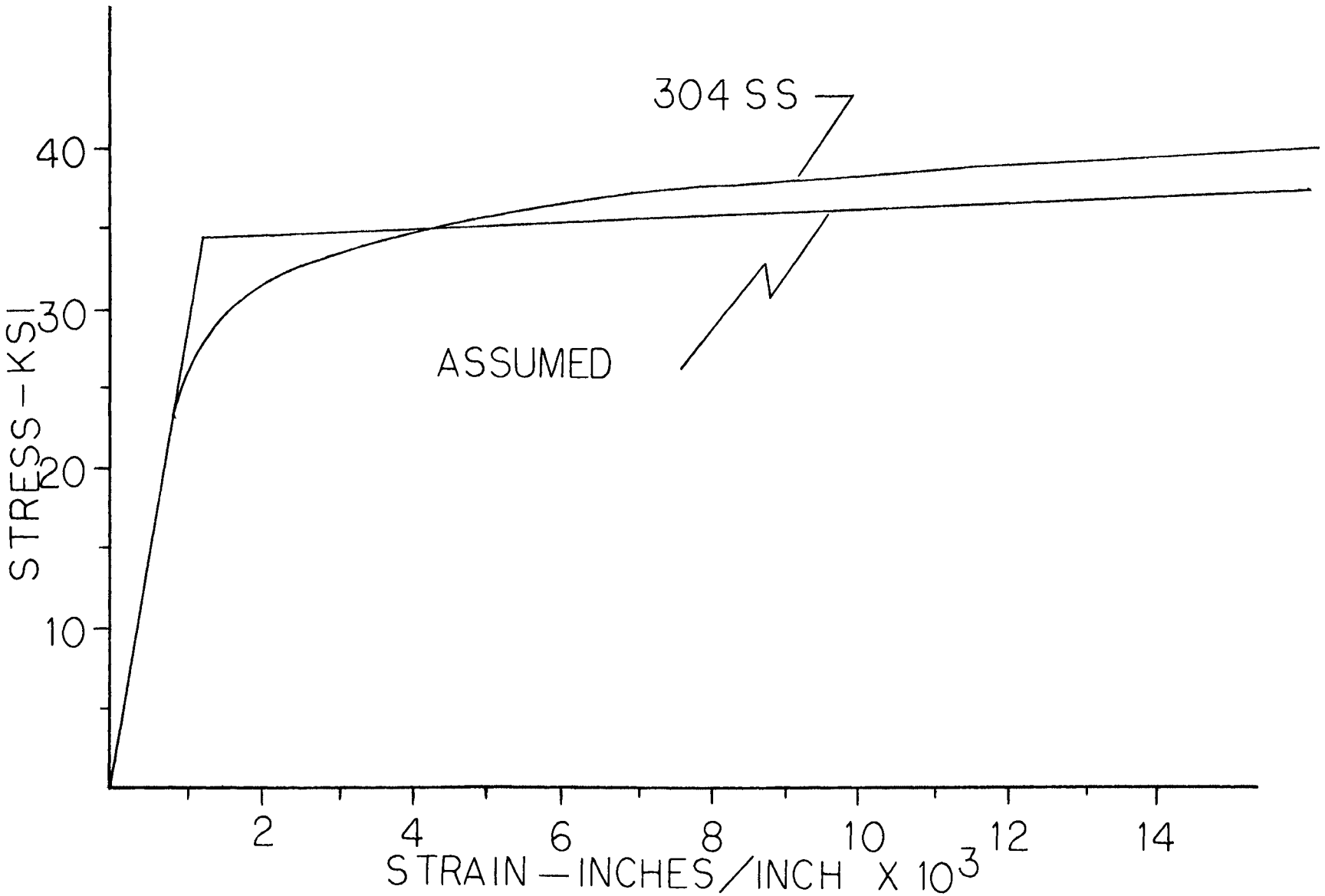

Figure 12 - Stress — Strain Curve for 304 SS and Curve used in Finite Element Analysis

load. It was therefore necessary to use a specimen material which had a low virgin yield strength and which could be loaded to stress levels of approximately twice its yield strength - the latter requirement being imposed to insure that the effects of prestraining were, at least, observable.

Isotropy is not necessary but such a characteristic would lessen the work required to determine the virgin yield surface. Initially, three materials were under consideration - Nittany No. 2 Brass, 304 stainless steel and ultra-pure ferritic transformer core iron. The most isotropic of these, the ferritic core iron, does not work harden to a sufficient level and consequently could not be loaded to twice its yield strength. Nittany No. 2 Brass, which was used by Hu to develop his bulge theory, also has limited work hardening capabilities and is the most likely of the three to be non-homogeneous and non-isotropic. As a consequence, 304 stainless steel was selected. The only attendant compromise with this material is the lack of homogeneity generated by the rolling process used to form the bar stock from which the parent specimens were cut.

Initial attempts to prestrain the stainless steel parent specimens showed that the stock was behaving as if it were not fully annealed. Hardness tests across the parent specimen cross-section showed a core hardness of R_B 87 and a lateral surface hardness of R_C 29. Further, a trial compression test of a parent specimen did not

generate a stress-strain curve that corresponded to the curve generated by a compression specimen cut from the core of the bar stock. As a result, all slugs underwent a second annealing and the parent specimen and core compression tests were repeated for comparison. These curves for the as-received annealed material and the double annealed material are shown in figure 13. No further heat treating was necessary and the slugs were prestrained in this condition.

The austenitic stainless steels, which include 304 stainless steel, are notorious for work hardening during machining operations. Since the prestrained parent specimens had to be cut up and machined into sub-specimens, great care was taken to insure that this characteristic did not enter the final data. Upon the advice of the producer of the specimen material, all machining was planned so that the final cut was 0.005 inches in depth. This left a work hardened zone of only 0.002 inches in depth which was too shallow to be of any consequence in the sub-specimens. In order to conform to the ASTM specifications for compression tests, the compression sub-specimens were machined to a size of 0.5 inches in diameter by 1.5 inches in length. The tension sub-specimens were 0.25 inches in diameter and 2.0 inches in length. The parent specimen and the sub-specimens are shown in figure 14.

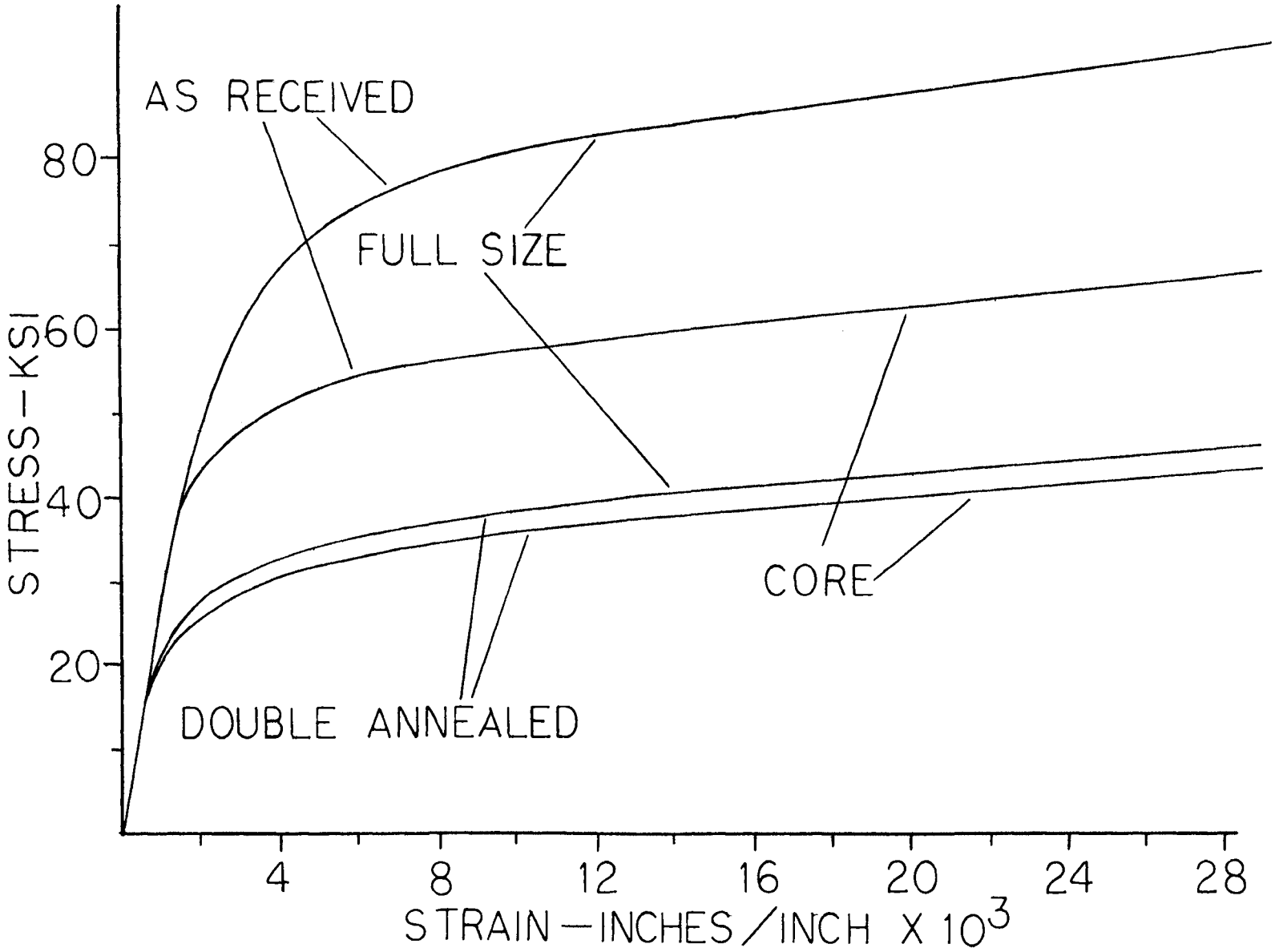

Figure 13 - Comparison of Stress — Strain Curves for the Double Annealed and As Received Materials

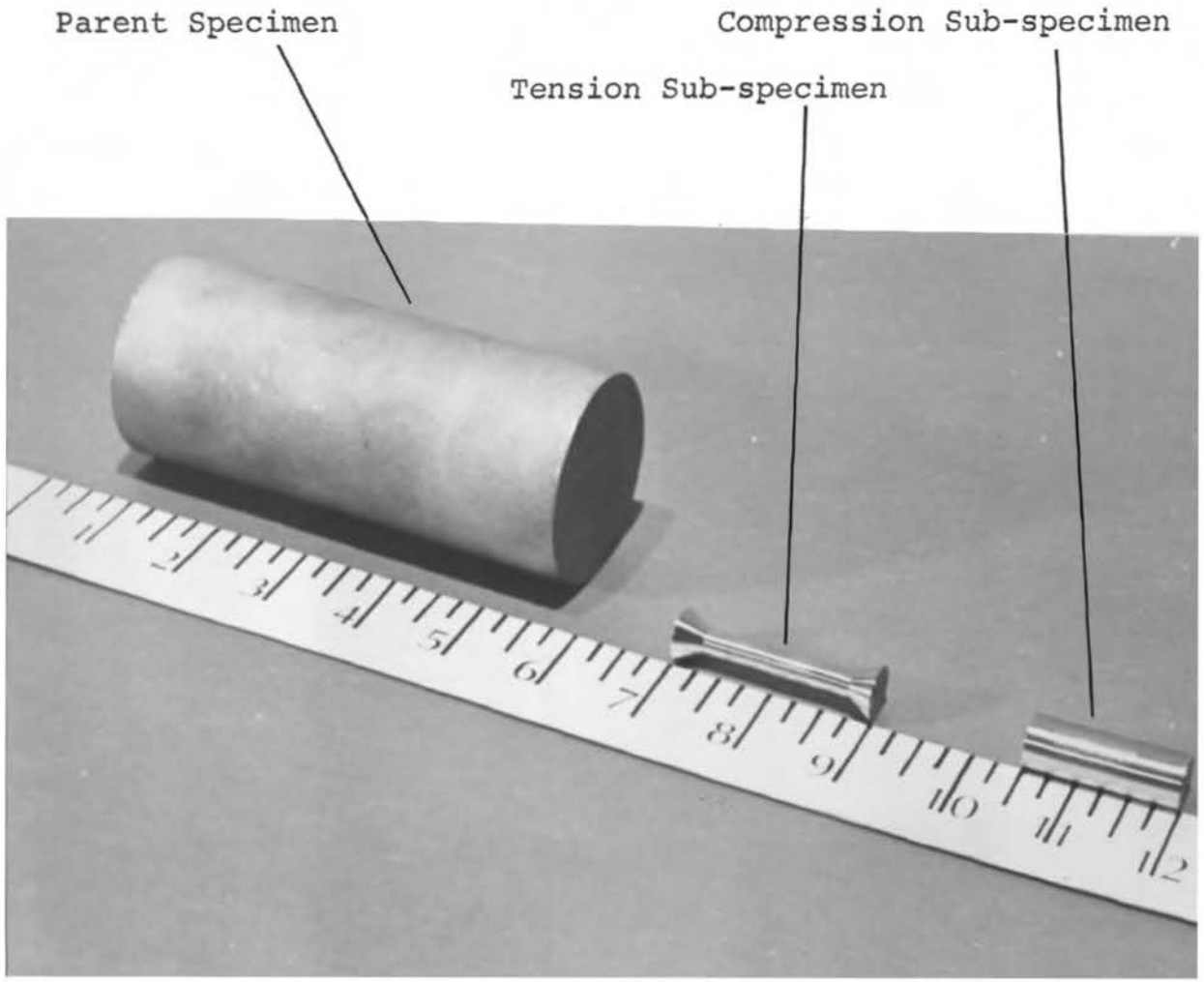

Figure 14 - Parent Specimen and Sub-specimens

C. Procedure and Apparatus

All of the prestraining and all of the sub-specimen tension and compression tests were conducted in thick-walled steel pressure vessels which were pressurized with aircraft hydraulic oil (MIL-H-5606). Although the oil is slightly compressible, the energy input to the fluid which is required for pressurization causes only slight changes in specimen temperature. Most of the heat generated by the pumping process is absorbed from the fluid by the vessel and the internal hardware. The consequent temperature rise in the specimen takes place during the vessel pressurization period and the apparent strain induced by any subsequent temperature change during the test is insignificant. This was checked, initially, by holding the vessel pressure for 15 minutes after pumping was stopped to check for strain indicator shifts. Shifts of less than 10 microinches/inch were noted. This indicated that the tests could be run without temperature compensation for the strain gages.

The use of resistance-type strain gages in high pressure environments has been examined in depth by Tien and Gordon[13], Gerdeen[14] and Milligan[15]. In accordance with the findings of these researchers, epoxy backed, constantan foil strain gages with 1/4 inch gage lengths were used to monitor strain levels in the specimens and internal load cells. These gages are reported to have gage factors which are unaffected by fluid environments up to approximately

140,000 psi. The gages were bonded with Eastman 910 contact adhesive and the installations were coated with multiple layers of nitrile rubber applied in an acetone solution. Removal of this rubber oil-proofing from the gages on selected specimens showed the compound to have excellent oil protection qualities.

Fluid pressure was supplied by an air operated differential piston-type pump and the pressure level was monitored by a manganin cell coupled to a specially calibrated Wheatstone bridge. The entire equipment set-up is shown in figure 15.

In order to protect the ram which was to be used for preloading the parent specimens, an operating limit of 240,000 pounds of ram load was set and each preloading operation was run to this level. Of this 240,000 lbs., approximately 173,000 lbs. were carried by the parent specimen. This corresponds to an axial stress in the center portion of the parent specimen of 55,000 psi - a value indicated by the final strain levels which were recorded. In addition, a 49,000 lb. component was generated by the 40,000 psi pressure environment and the remaining 18,000 lb. component was due to seal friction drag.

Strain gages were mounted at the extreme ends of the 2.5 inch parent specimen center section to insure that the upper and lower contact blocks did not cause any undesirable variations in end effects. This also was an effective means of insuring that each parent specimen was prestrained

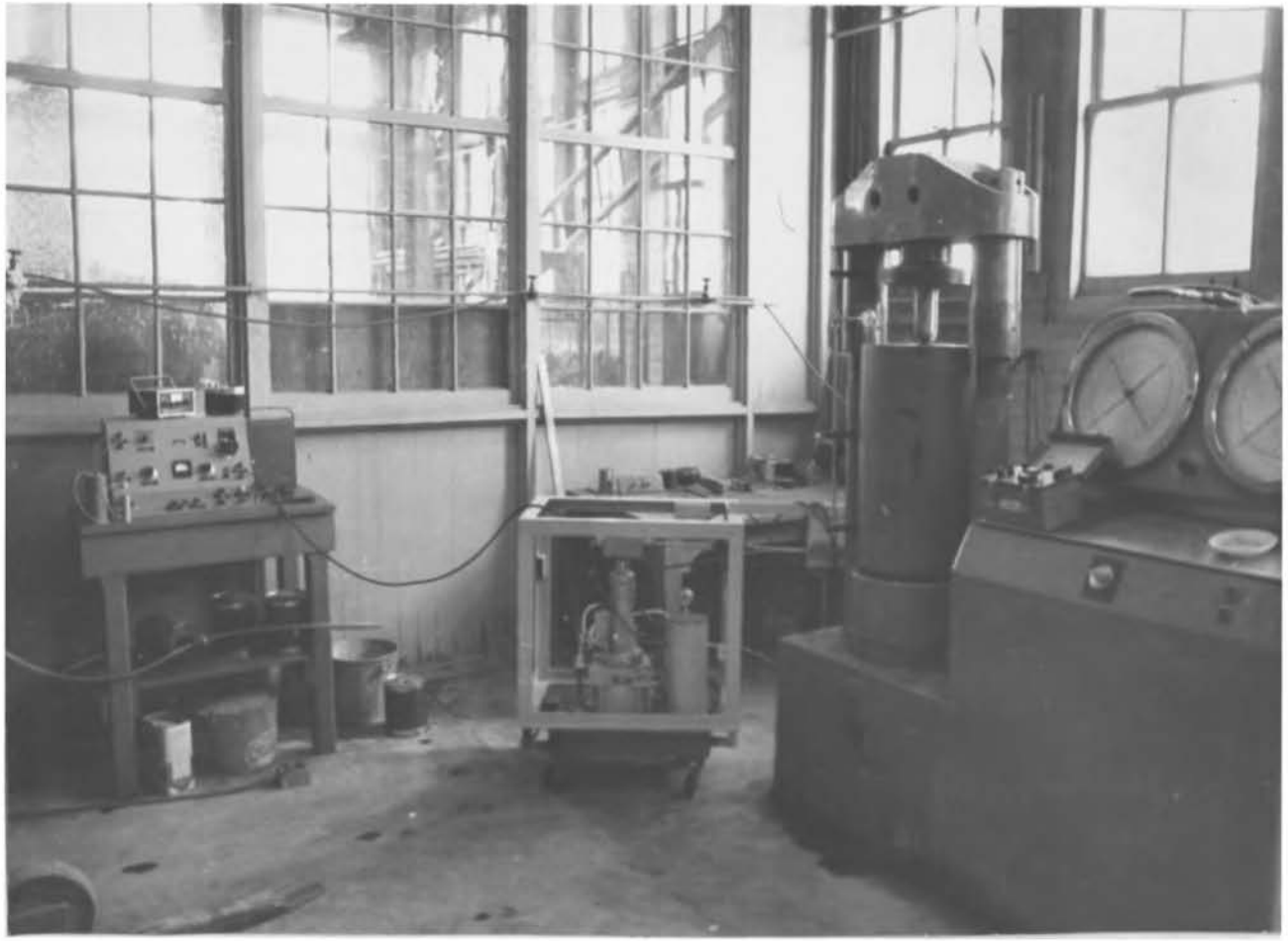

Figure 15 -- Overall View of Laboratory Set-up

to the same level - not only was ram load duplicated from test to test, but strain levels were also checked. At the final ram load, a strain level of 45,000 microinches/inch was common, but variations of up to 8 percent of this value were seen. This could, if the instrumentation was perfect, represent a variation in prestress level of 2,375 psi about the nominal value of 55,000 psi. Undoubtedly, some of the final strain level variations from slug to slug were due to minor variations in the performance of each individual gage installation. A view of the internal vessel hardware used to prestrain the parent specimens appears in figure 16.

Following the prestraining, the parent specimens were allowed to sit at room temperature for three weeks to accommodate any relaxation effects in the microstructure that might occur. After this, the ends were removed from the parent specimens and the center section was either quartered or cut into disks depending on whether the specimen was to provide longitudinal or transverse sub-specimens. The longitudinal sub-specimens were turned directly from the quarter sectors. Each disk was trimmed so that a sub-specimen could be turned from along a diametral axis. Cutting depths and feed rates were adjusted so that the material did not heat-up appreciably.

The sub-specimen tension tests were accomplished by means of the load reversing yokes shown in figure 17, and the specimen extenders shown in figure 18. The yokes simply allowed the compressive ram loads to develop tensile

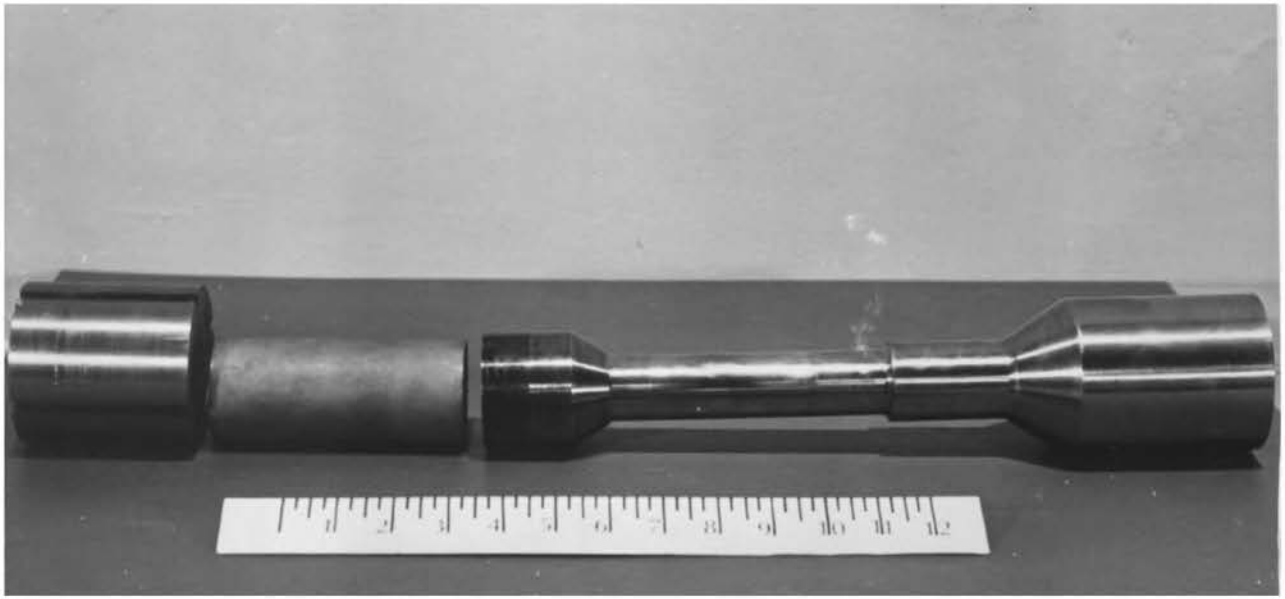

Figure 16 - Internal Vessel Hardware used for Parent Specimen Prestraining

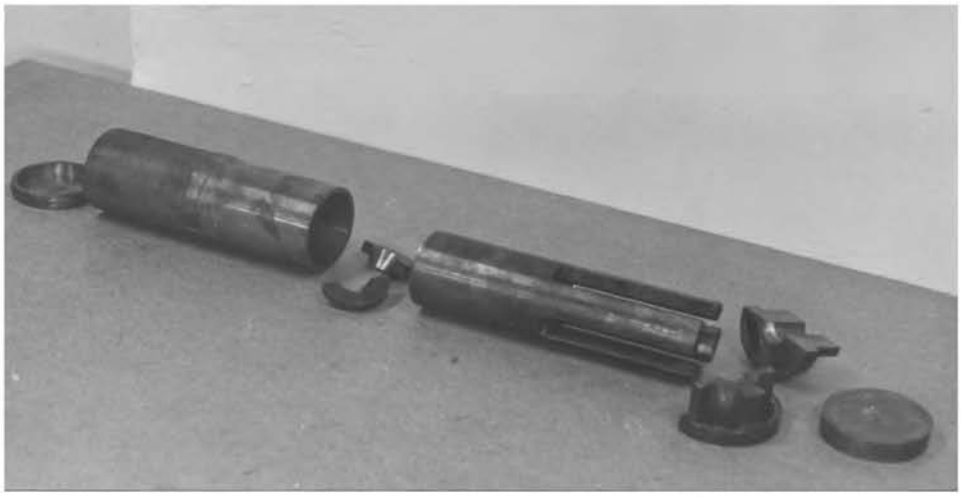

Figure 17 - Load Reversing Yokes

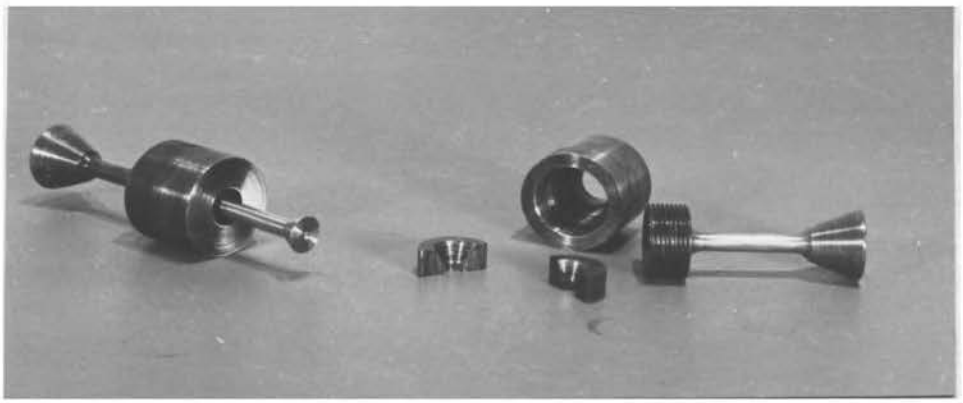

Figure 18 - Specimen Extenders

forces. The extenders, which were used to grip the ends of the tension sub-specimens, served two purposes - they adapted the small tension specimens to load reversing yokes which had been designed for much larger specimens, and one of the extenders was instrumented to serve as a load cell. An internal load measuring capability was necessary because of the low loads which were required to yield the tension sub-specimens. An external scheme for specimen load measurement would be subject to great error if the ram seal drag or vessel pressure varied slightly during the test. Since the extenders were made from 300 grade maraging steel, the load cell gave a linear response to load levels far beyond that required to perform the test. Frequent recalibration throughout the tension sub-specimen testing program showed no change in the calibration curve.

The sub-specimen compression tests were done in two different vessels. In order to save time and effort the tests conducted in an environment at or below 40,000 psi were performed in a vessel which was considerably lighter and smaller than the vessel described previously. This light-weight vessel had a 0.75 inch diameter ram and a special low-drag ram seal which permitted external measurement of the load on the compression sub-specimen. The specimen load was taken as simply the total external ram load minus the seal friction drag and the force component due to the pressurized fluid. The combined

seal drag and pressure force was determined for each test run by adjusting the loading head speed to match the nominal speed used during the test and then noting the force required to move the ram into the vessel. This force was monitored prior to each test at a time when the loading ram was not yet in contact with the specimen. Specimen alignment was insured by shallow recesses machined into the plattens which were used to apply the loads. The light-weight vessel and related internal hardware are shown in figure 19.

The remaining compression tests were performed in the high pressure vessel which was used for the prestraining and the tension sub-specimen tests. The difficulty of inserting and properly positioning a small compression specimen in the relatively large cavity of this vessel prompted the construction of a module which could be assembled outside of the chamber and simply dropped in. This module consisted of an aluminum cylinder which contained a movable hardened steel piston and a specimen support pedestal which was fixed in the lower end of the cylinder. The specimen was held between the lower support pedestal and the movable piston which protruded through the top of the cylinder. This movable piston contacted the vessel ram. The specimen support pedestal was instrumented for use as a load cell and the performance of this load cell was comparable to that of the tension load cell. The compression module is shown in figures 20 and 21.

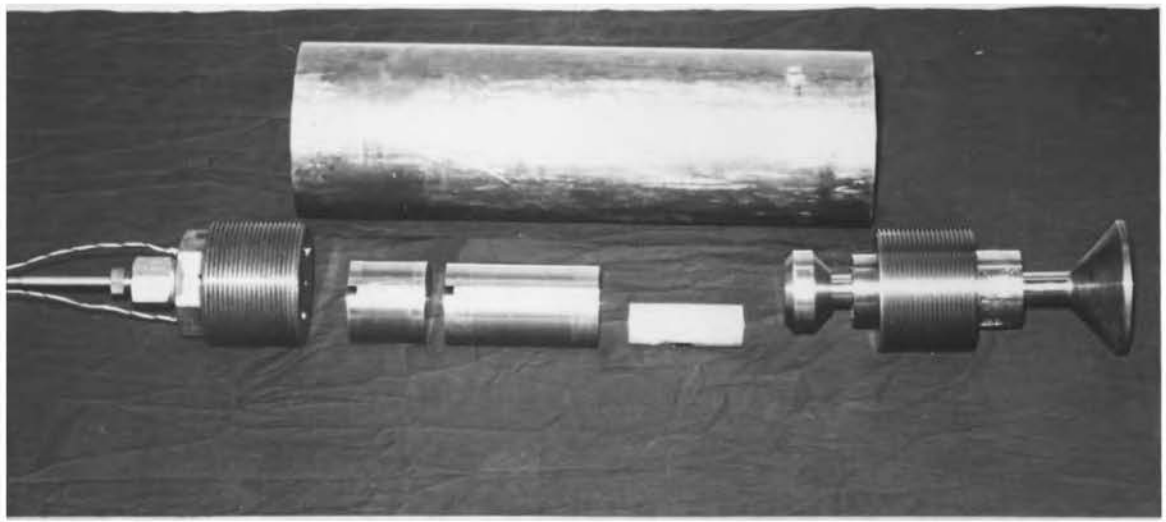

Figure 19 - Light-weight Vessel and Internal Hardware

Figure 20 - Assembled Compression Module

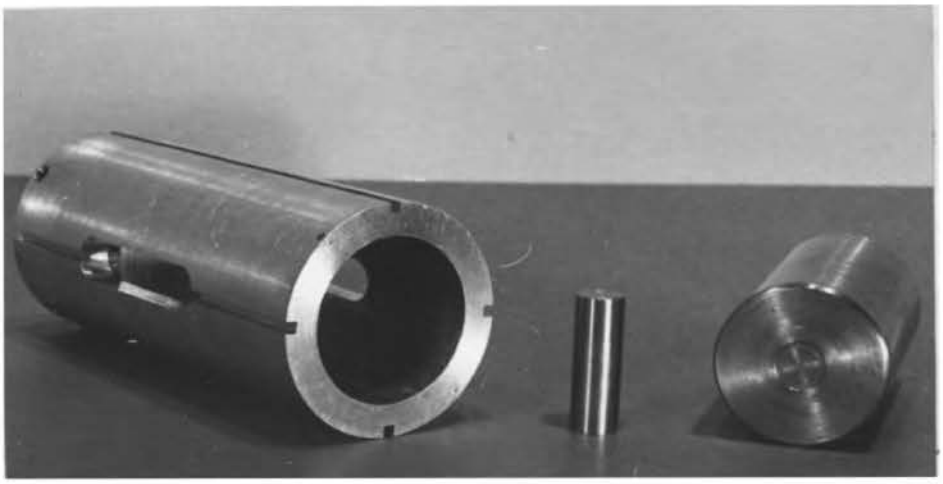

Figure 21 - Compression Module with Specimen and Piston Removed

IV. RESULTS

A. Experimental Data

The first step in the data reduction process was to select an appropriate definition for yielding. For a material such as a low carbon steel where yielding is pronounced, this would not be a problem, but such is not the case with any austenitic stainless steel. As a result of discussions with Pugh[16], three possibilities were considered. These definitions of yielding are illustrated on a fictitious stress-strain curve in figure 22. The first was that of defining the proportional point as the yield point. Point A represents the proportional point in figure 22. This was immediately abandoned since the proportional point is extremely low, if it exists at all, for 304 stainless steel. The second definition involves extending the elastic and plastic slopes of the curve until they intersect, as at point B in figure 22. The resulting bi-linear stress-strain curve does not even closely approximate the stress-strain curve generated by the tension sub-specimens and, although the fit for the compression sub-specimen stress-strain curves is somewhat better, this case is not good either.

Finally, the conventional offset method was selected. It was assumed that the material would unload along a path parallel to the initial elastic slope of the stress-strain curve and such a path was constructed from a point on the abscissa which represents the amount of allowable permanent

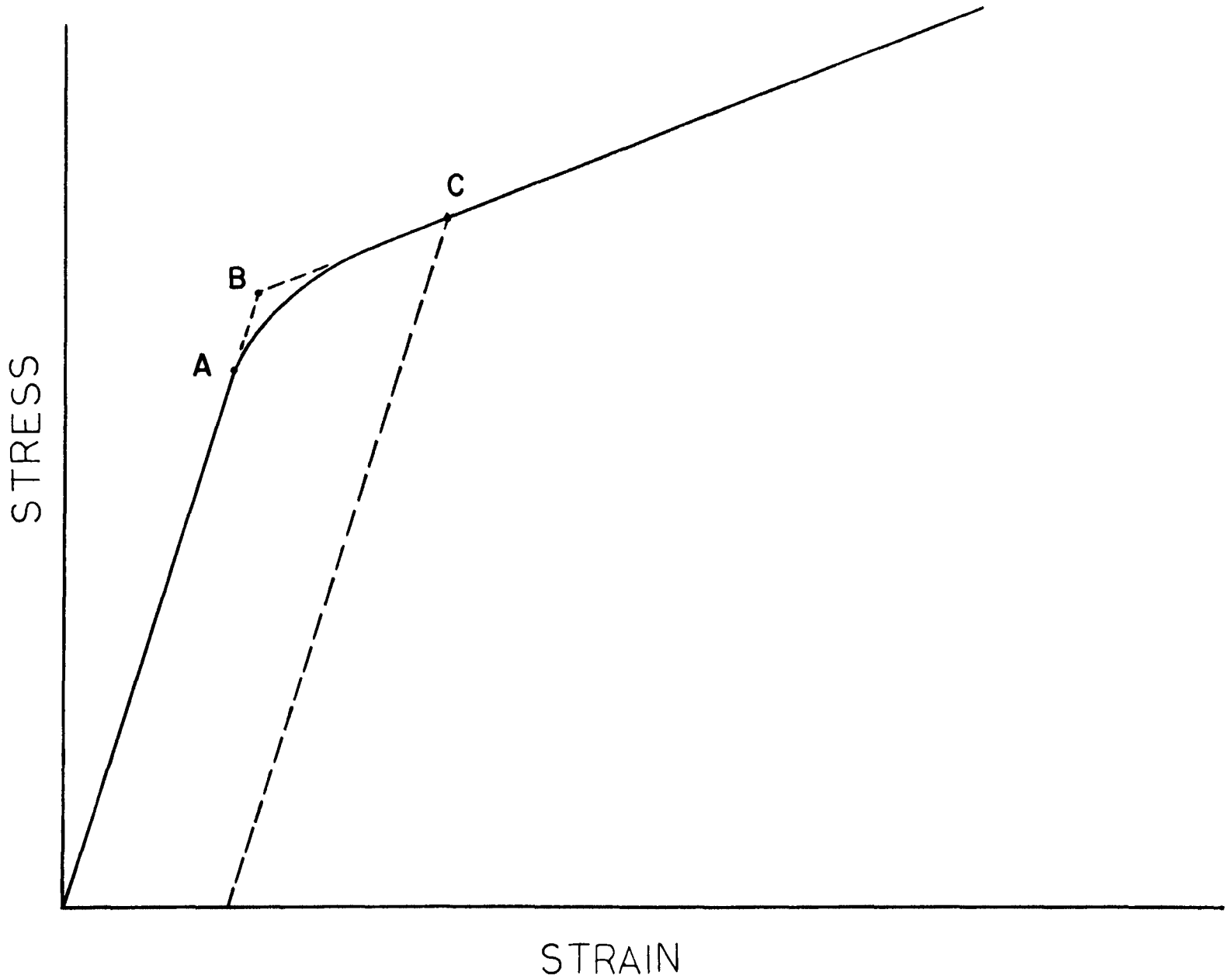

Figure 22 - Illustration of Various Definitions of Yielding

plastic strain. The intersection of this unloading path and the stress-strain curve - point C on figure 22 - was assumed to define the yield strength. Although the amount of allowable plastic strain is quite arbitrary, convention dictates the use of 0.2 percent plastic strain with longitudinal stress-longitudinal strain curves.

The 0.2 percent offset method was applied to the classical longitudinal stress-longitudinal strain curves that were constructed for each sub-specimen test. If it is assumed that Poisson's ratio is constant up until yielding occurs, this method yields results identical to those obtained by using an effective stress-effective strain plot with the allowable permanent effective strain reduced to 2/3 $(1 + \mu)$ of the amount permitted in the case of the longitudinal stress-longitudinal strain curves. The effective stress is defined as

$$\bar{\sigma} = \frac{1}{\sqrt{2}} \left[\left(\sigma_1 - \sigma_2 \right)^2 + \left(\sigma_2 - \sigma_3 \right)^2 + \left(\sigma_3 - \sigma_1 \right)^2 \right]^{.5} \qquad (1)$$

and effective strain is defined

$$\bar{\varepsilon} = \frac{\sqrt{2}}{3} \left[\left(\varepsilon_1 - \varepsilon_2 \right)^2 + \left(\varepsilon_2 - \varepsilon_3 \right)^2 + \left(\varepsilon_3 - \varepsilon_1 \right)^2 \right]^{.5} \qquad (2)$$

The elastic modulus was found by determining the slope of the stress-strain curve at the origin. The slope value was found to be approximately 30×10^6 psi for all cases, and this value did not change with pressure environment. Further, the shape of the stress-strain curves for each of

the particular types of tests, i.e., longitudinal tension, transverse compression, etc., did not vary with the pressure environment changes. Typical stress-strain curves for longitudinal tension and compression are shown in figure 23, and the typical curves for transverse tension and compression are shown in figure 24. It should be noted that these curves do not extend to fracture.

The yield strength values obtained in a direction opposite to that of prestraining were never lower than the values for the same case in the virgin material. This tends to mask the manifestations of the Baushinger effect in this material. However, it is immediately obvious after comparing the tension and compression curves in figure 23 with the virgin curve in figure 12 that the compressive longitudinal prestraining caused the stress-strain curves for the longitudinal tension sub-specimens to "bend over" early. The definition of yielding as used in this project is the reason why this "bend over" phenomena does not have a great influence on the subsequent yield data.

The data representing the tests of all the longitudinal sub-specimens appear in figure 25. Each point represents a conventional yield strength plotted against the pressure level present in the material when yielding occurred. For this purpose, pressure is defined as the negative of the spherical component of the stress state, or

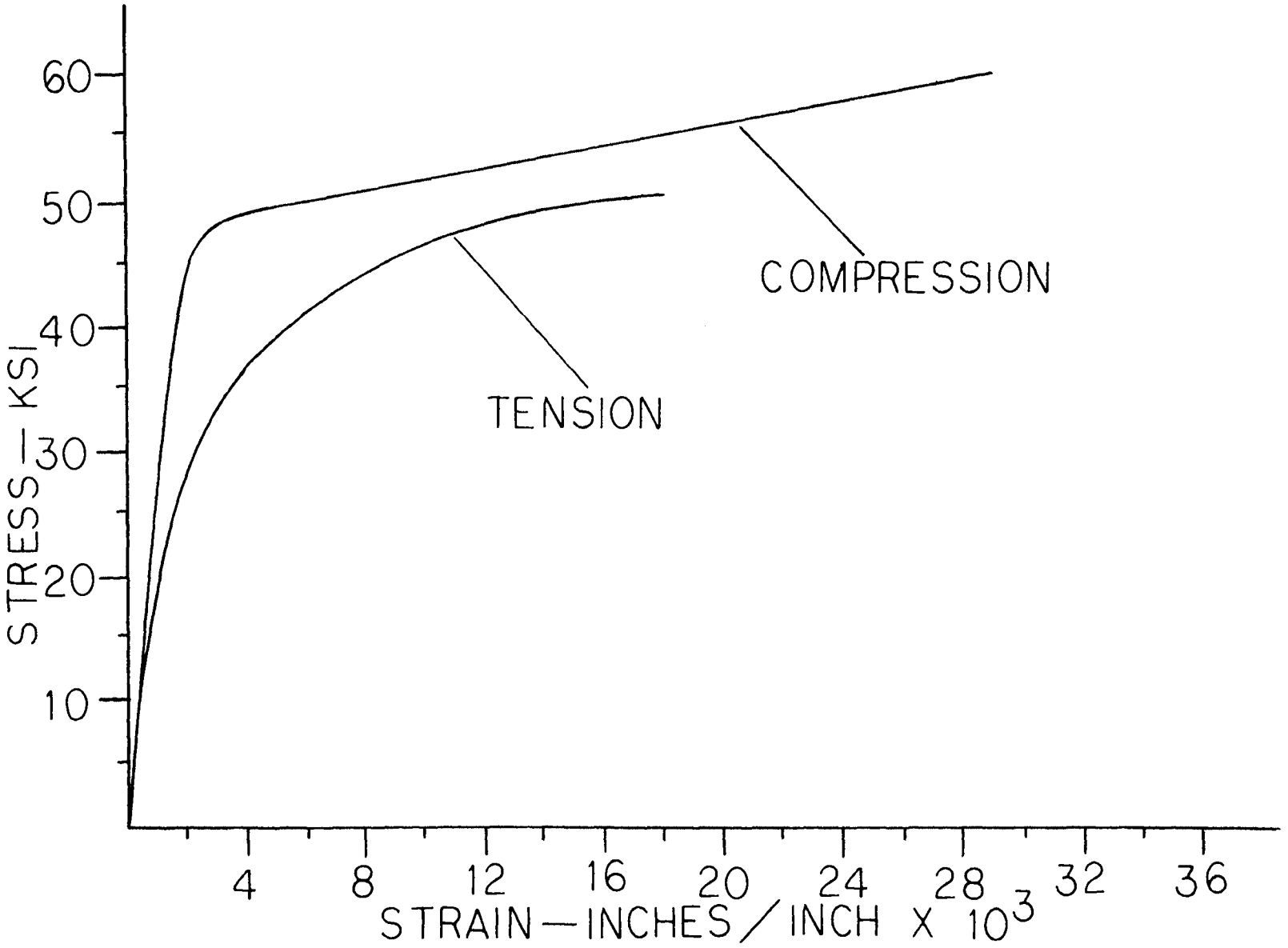

Figure 23 - Stress — Strain Curves for Longitudinal Sub-specimens

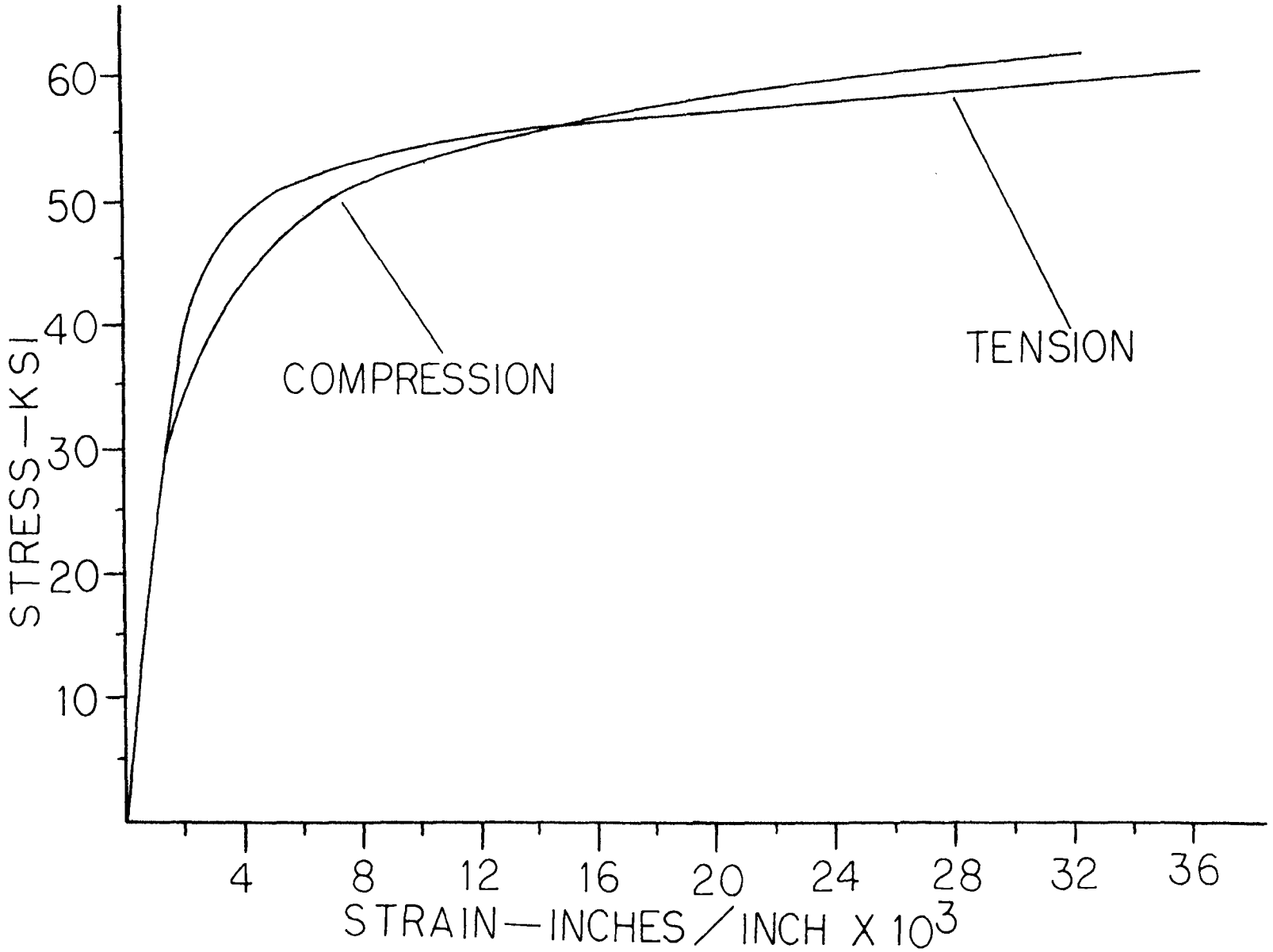

Figure 24 - Stress — Strain Curves for Transverse Sub-specimens

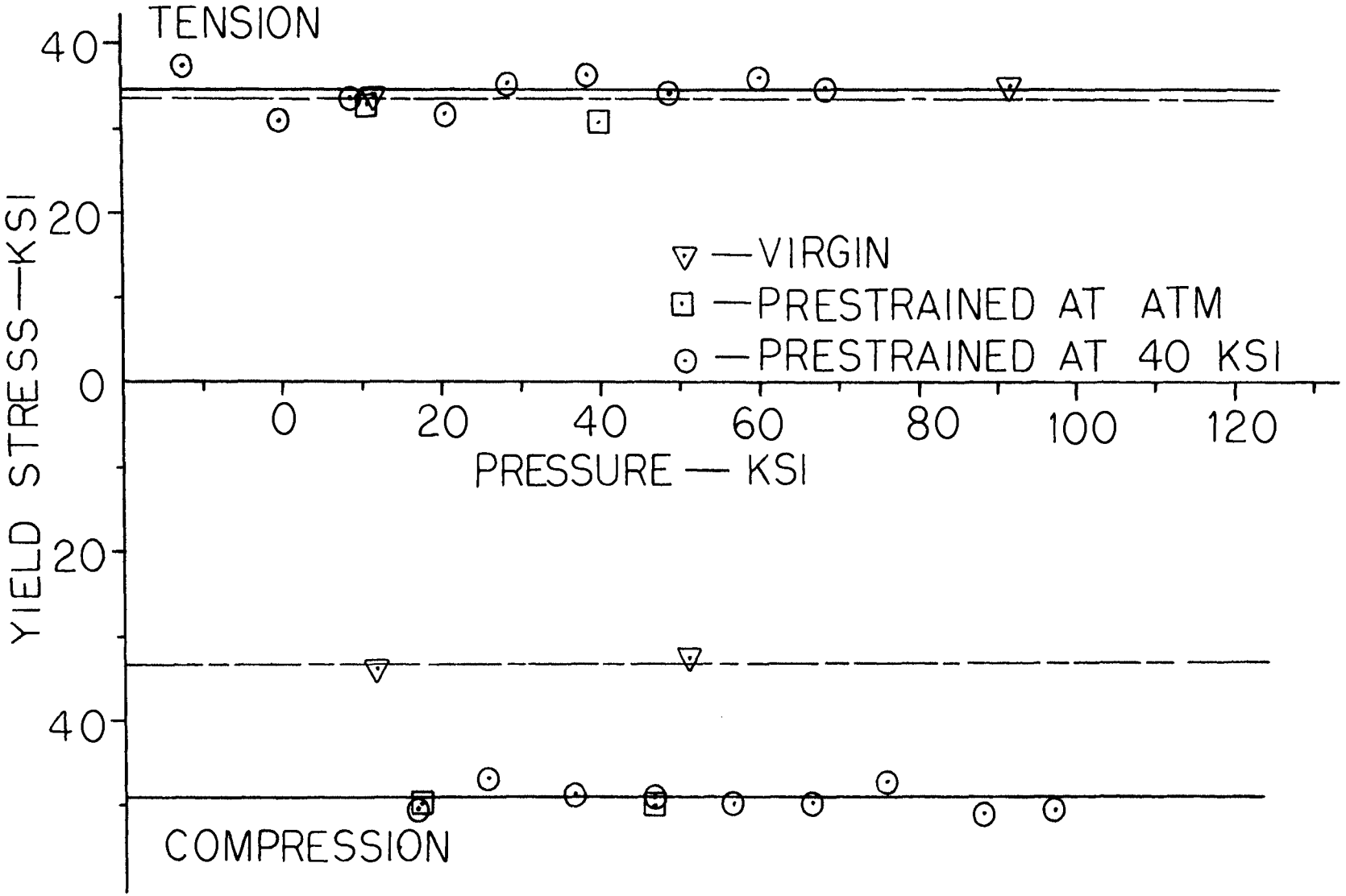

Figure 25 - Longitudinal Sub-specimen Yield Data

$$P = -\frac{(\sigma_1 + \sigma_2 + \sigma_3)}{3} \qquad (3)$$

In effect, this plot represents an expanded view of the intersection of the subsequent yield surface and the σ_1— hydrostatic axis plane. The straight lines representing the yield surface are drawn parallel to the hydrostatic axis through the numerical average of the yield strengths. Attempts to fit straight lines to the data points via the least-squares technique shows this to be a reasonable representation of the data. The lines between the hydrostatic axis and the subsequent yield data, represent the virgin yield conditions. It is this plot that best illustrates the independence of the yield strength of 304 stainless steel on pressure. It is evident that the prestraining resulted in a large gain in yield strength in the direction of the prestraining while in a direction opposite to that of the prestraining very little was gained. The increases in yield strengths for these two cases are, respectively, 16,300 psi and 1,300 psi.

The four points that represent data obtained from specimens that were prestrained in atmosphere give good agreement with the remaining points. This indicates that 304 stainless steel has the same subsequent yield surface for a given type and degree of prestrain for at least two different prestraining pressure environments. In light of these data, it is reasonable to expect that the com-

pressive pressure environment used for the prestraining operations has no influence on the subsequent yield surface. The shape of the virgin yield surface in the region of high tensile pressure environments has not been determined by experiments at this date, hence, omission of this region in the discussion is understandable. The prime reason for the lack of a complete spectrum of tensile data is the unavailability of suitable triaxial tension test specimens.

The data representing the tests of all the transverse sub-specimens appear, similarly, in figure 26. This plot represents an expanded view of the intersection of the subsequent yield surface and either the σ_2-hydrostatic axis plane or the σ_3-hydrostatic axis plane. Once again, the lines drawn parallel to the hydrostatic axis through the data are in close agreement with the least-squares predictions. This plot shows that the longitudinal prestraining enhanced the yield strength in both the direction of transverse tension and the direction of transverse compression. Increases in these directions are 14,200 psi and 9,300 psi, respectively.

Finally, the results of figures 25 and 26 are combined to form a view of the yield surface as seen by looking down the hydrostatic axis. This view is shown in figure 27. The lines drawn through the data points in figures 25 and 26 now appear as points in the deviatoric plane. Although the non-isotropic characteristics generated by the prestrain-

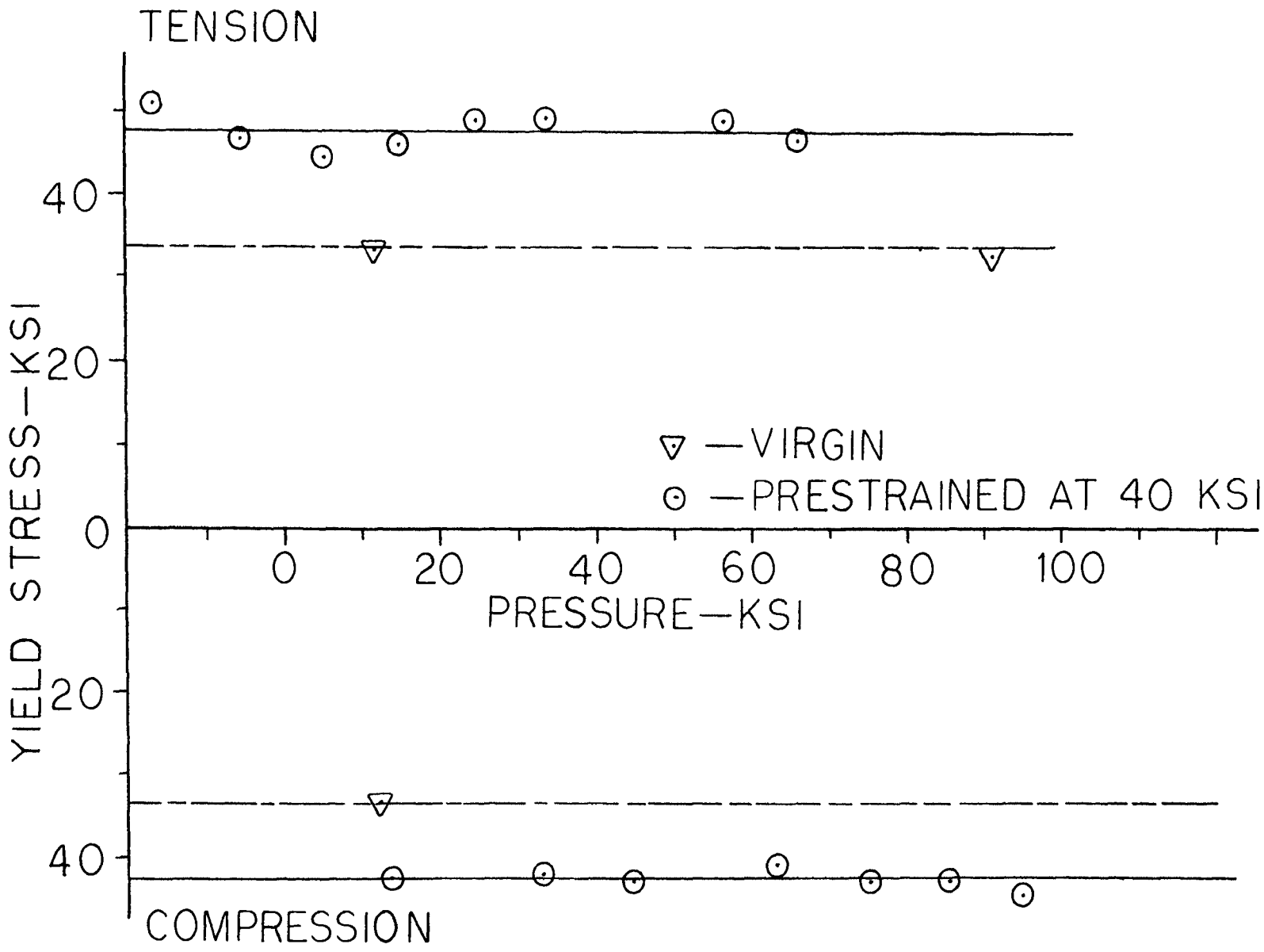

Figure 26 - Transverse Sub-specimen Yield Data

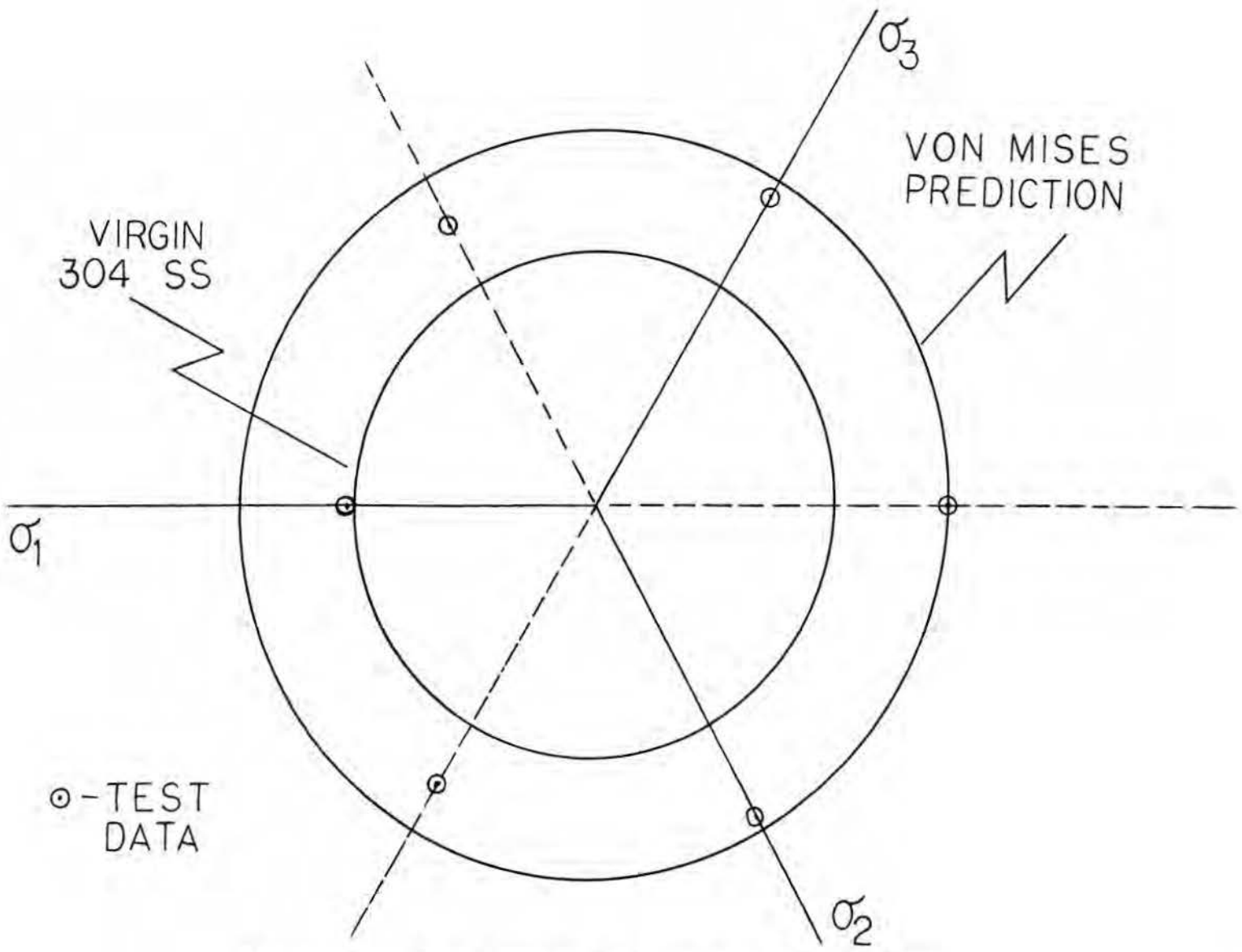

Figure 27 - Test Results Seen in Deviatoric Plane

ing have caused the yield surface to shift in the direction of prestraining, the new yield surface still completely contains the virgin surface since the surface has simultaneously expanded outward. The von Mises subsequent yield surface for this case completely contains the empirical surface.

B. Theoretical and Practical Considerations

It is immediately obvious that the empirical subsequent yield surface does not behave according to the prediction of any of the previously mentioned theories. Some of these theories were put forth because of mathematical simplicity - a concept worth striving for when rapid calculations must be made to check for yielding without the aid of high speed computation machinery. To some extent, this simplicity has been preserved in several of the mathematical yield locus representations which follow. Although the profile as seen in the π-plane is not circular, circles can be fitted which will describe the yield condition with varying degrees of conservatism.

In the particular case investigated here, we can observe that the prestraining resulted in a 16,300 psi increase in compressive yield strength and a 1,300 psi increase in tensile yield strength along the direction of prestraining. Since this effect is independent of hydrostatic pressure level, we can use these two pieces of information to construct some yield surfaces that approximate the empirical surface. Consider, for example, the π-plane section shown in figure 28. This circle represents a yield condition which is conservative with respect to the experimental data in all cases. The circle can be constructed simply by increasing the radius and shifting the origin of the virgin yield surface by amounts equal to

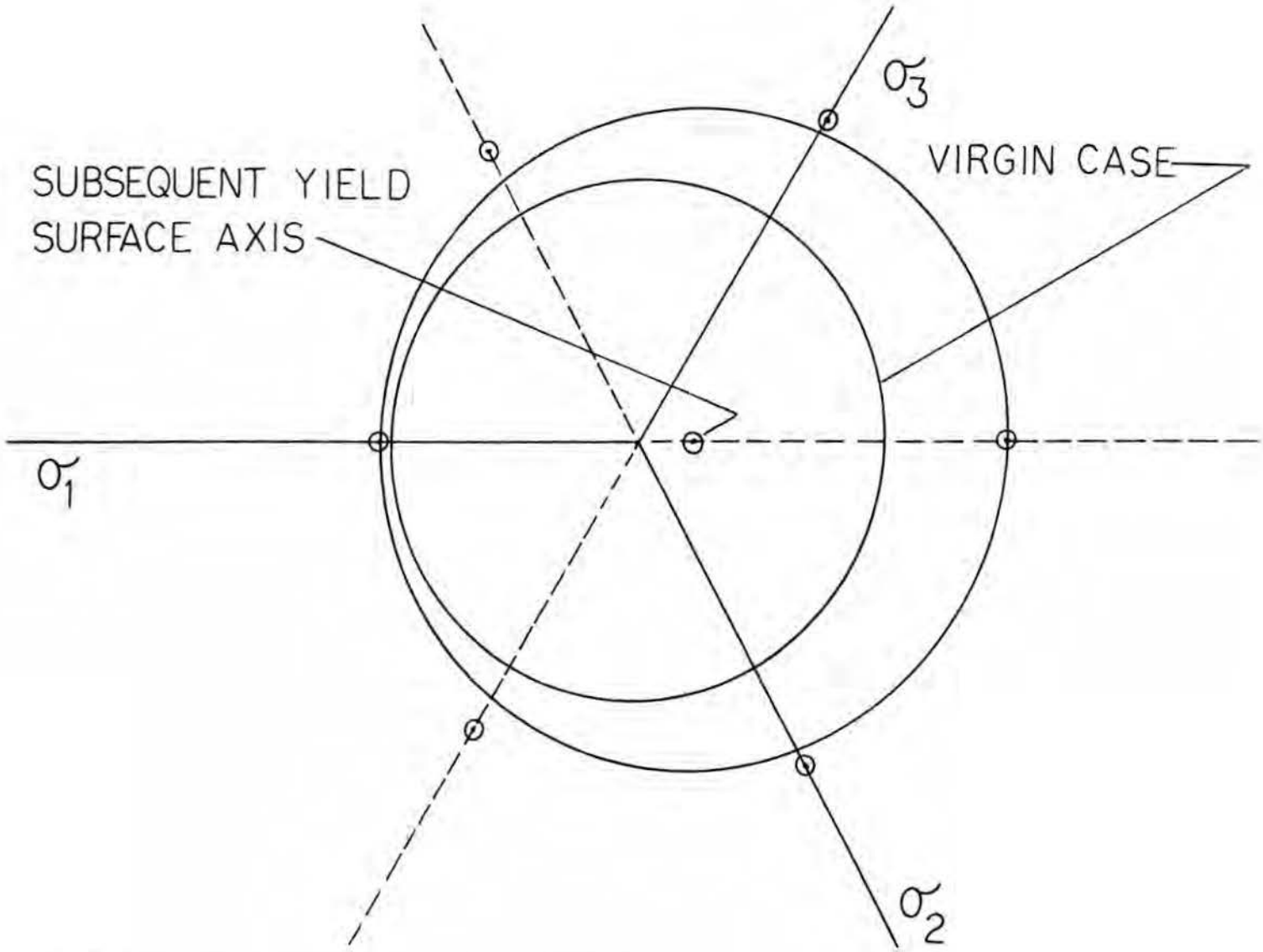

Figure 28 - Conservative Yield Surface Approximation using a Circular Section

$0.54\sqrt{2/3}$ and $0.46\sqrt{2/3}$ times the increase in effective stress at yield in the direction of prestrain. Thus, the new π-plane section can be derived from one simple test which tells the increase in yield strength in the direction of prestraining. This theory can easily accommodate different degrees of prestraining. An example of the predicted π-plane section resulting from compressive prestraining of 304 stainless steel to a level of 80,000 psi appears in figure 29.

If one were willing to perform an additional test, i.e., determining the increase in yield strength achieved in a direction directly opposite to that of prestraining, the same circle could then be based on two data points - a situation which is much more desirable for the extrapolation of the theory to different degrees of prestrain. These two points would establish the diameter and position of the desired π-plane circle. The degree of shift of the axis of the yield cylinder could then easily be determined.

Accepting a lesser degree of conservatism in developing a yield model which approximates the data will give a better fit to the points in the π-plane which outline the experimental contour. Such a curve appears in figure 30. In a manner identical to the first example, this circle can be constructed by increasing the virgin yield circle radius by an amount equal to $.65\sqrt{2/3}$ of the effective stress increase at yield achieved in the direction of prestraining

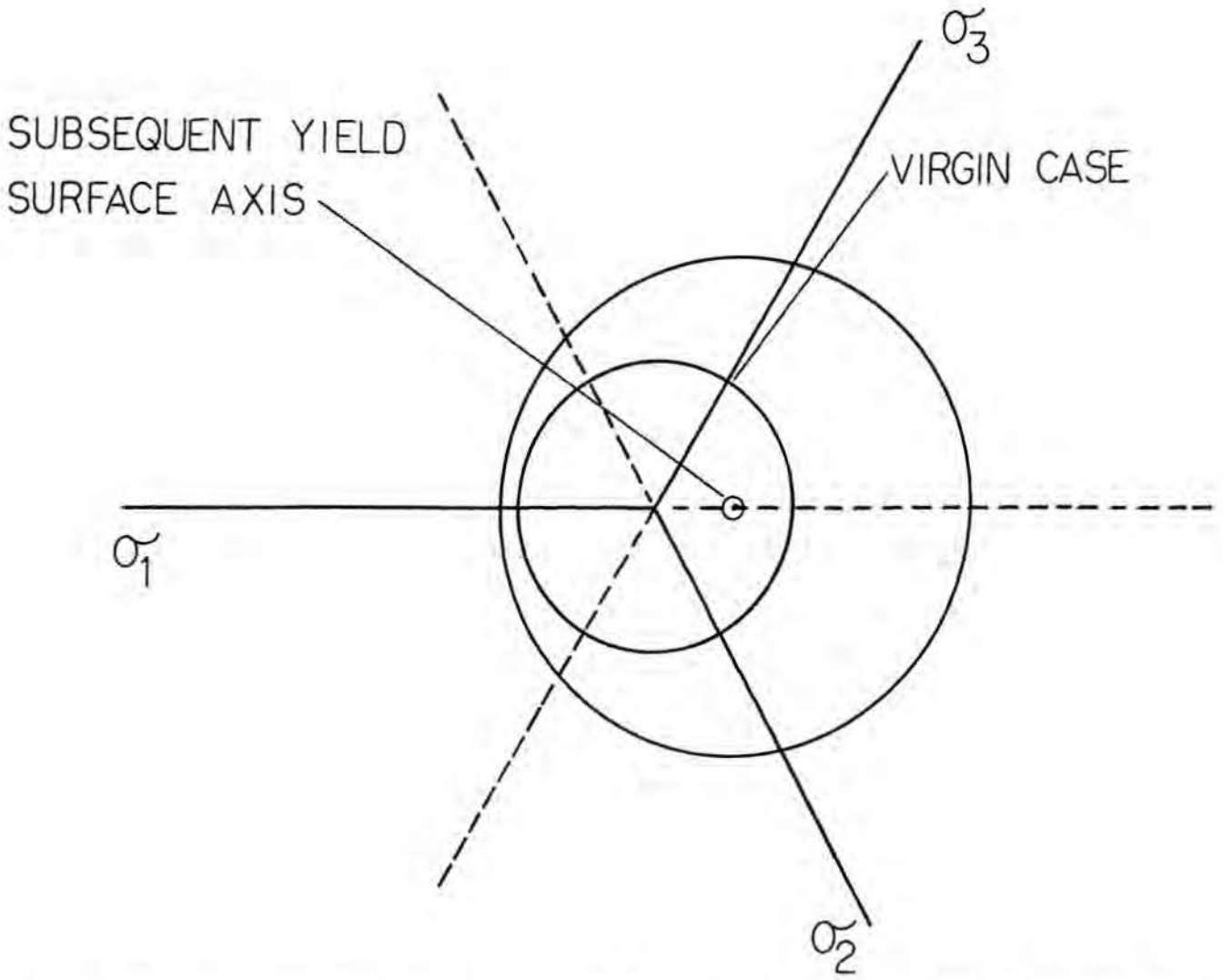

Figure 29 - Conservative Yield Surface Approximation Extended to 80,000 psi Prestress

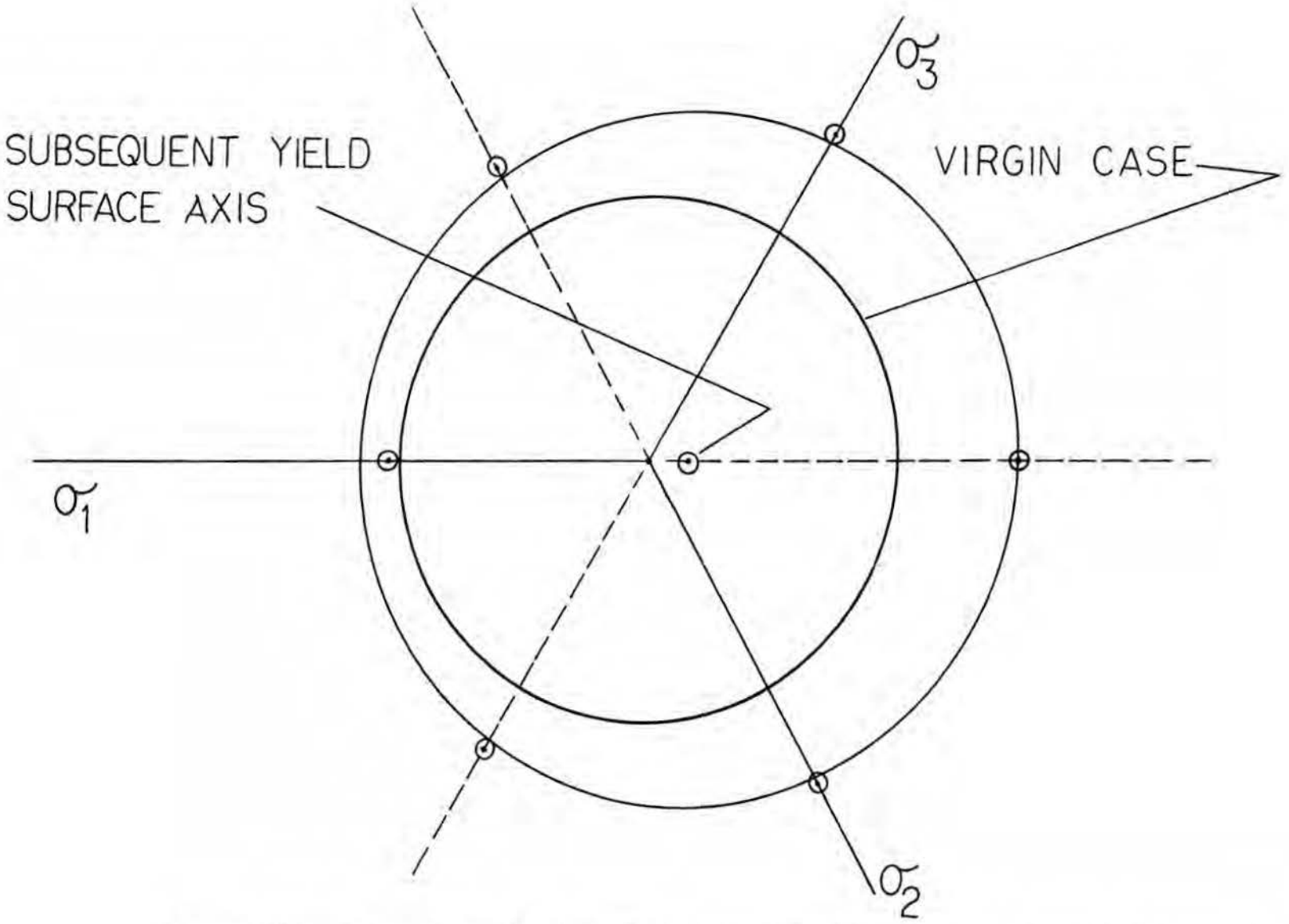

Figure 30 - Close-fit Yield Surface Approximation using a Circular Section

and then by shifting the circle in the direction of pre-straining by an amount representative of the remainder of this effective stress increase. Whether this representation or the representation shown in figure 28 is chosen for a particular application depends on the nature of the problem under consideration. The subsequent yield locus shown in figure 28 would be preferable, for example, if the application concerned uniaxial cyclic tension-compression. The subsequent yield locus shown in figure 30 is desirable for problems in which the effective stress probe lies anywhere in the deviatoric plane except near the positive σ_1 axis.

The advantages of fitting a cylindrical surface to the experimental data centers around the ease with which such a yield surface can be applied to problems. The von Mises yield condition is written as

$$\frac{1}{2}\left[\left(\sigma_1 - \sigma_2\right)^2 + \left(\sigma_2 - \sigma_3\right)^2 + \left(\sigma_3 - \sigma_1\right)^2\right] = \sigma_o^2 \qquad (4)$$

where σ_o is the yield strength in simple tension. Equation (4) is the equation of the cylindrical yield surface which has the hydrostatic axis as its axis of symmetry. It is easy to modify this equation to fit the curves proposed earlier in this section. For example, if σ_o is taken as the virgin 304 stainless steel yield strength and the material is loaded to a level of σ_o' along the σ_1 axis, the

shifted and expanded yield cylinder can be written simply

$$\frac{1}{2}\left[\left(\left(\sigma_1-S\right)-\sigma_2\right)^2+\left(\sigma_2-\sigma_3\right)^2+\left(\sigma_3-\left(\sigma_1-S\right)\right)^2\right]=\left(\sigma_o+R\right)^2 \quad (5)$$

where

$$S = .46\left(|\sigma_o'|-\sigma_o\right) \quad (6a)$$

and

$$R = .54\left(|\sigma_o'|-\sigma_o\right) \quad (7a)$$

If σ_o' equals -49,500 psi, and since σ_o equals 33,200 psi, equation (5) represents the subsequent yield criterion for 304 stainless steel first proposed in this section. The alternate, or less conservative, proposal can be accommodated simply by changing equation (6a) to

$$S = .35\left(|\sigma_o'|-\sigma_o\right) \quad (6b)$$

and equation (7a) to

$$R = .65\left(|\sigma_o'|-\sigma_o\right) \quad (7b)$$

A final representation of the experimental data is the exact-fit polynomial curve shown in figure 31. If one

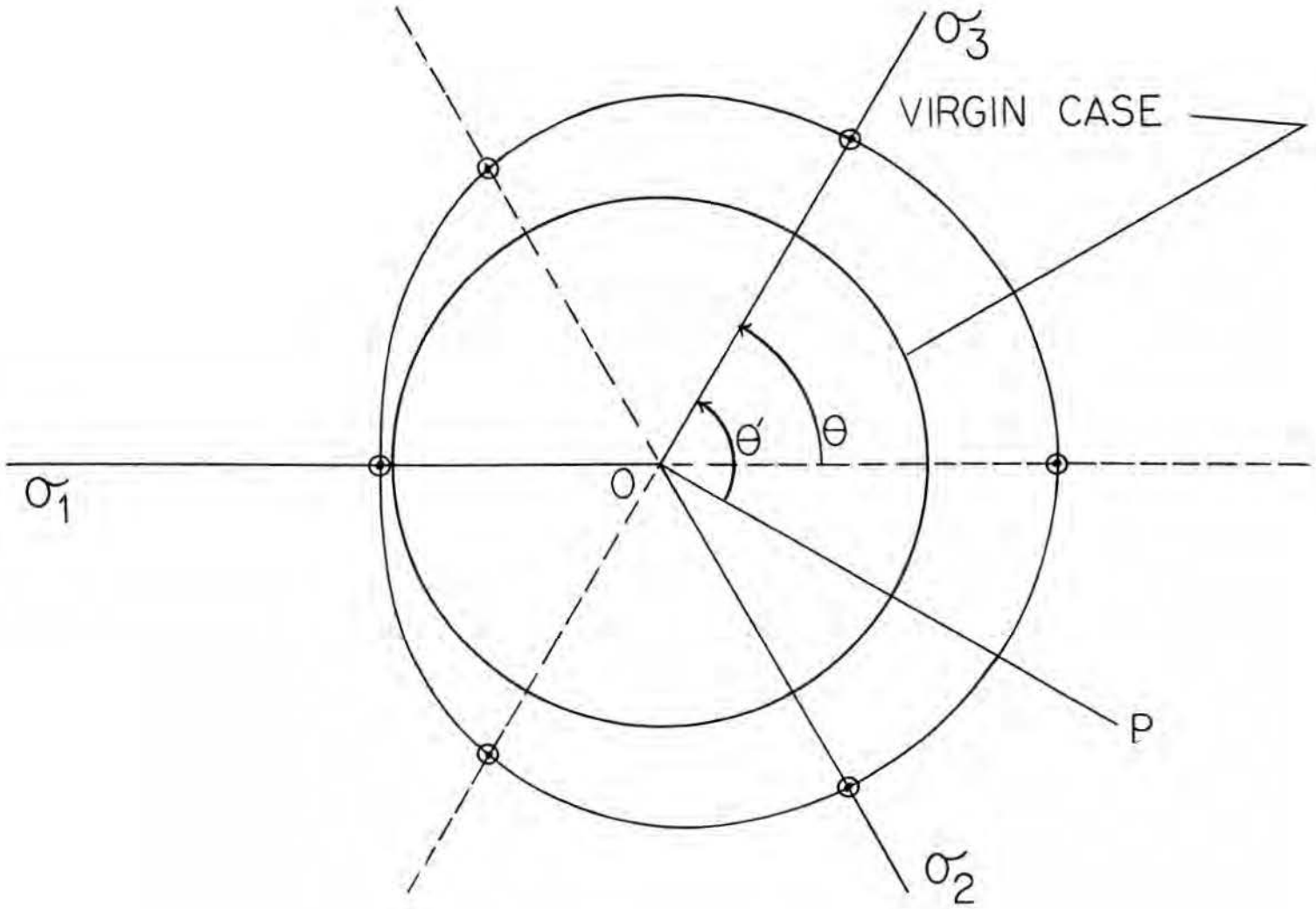

Figure 31 - Yield Surface Approximation Generated by a Polynomial Curve Fit

references the angle θ to the axis of prestraining, the radial distance, r, from the hydrostatic axis to the subsequent yield surface can be expressed as

$$r = \sqrt{2/3}\, r'(\theta) \tag{8}$$

where $r'(\theta)$ is the magnitude of the effective stress vector required to produce yielding if the stress state lies in the θ direction. Due to the symmetry assumed with respect to the axis of prestraining, the following conditions must hold

$$r'(0) = 49{,}500 \text{ psi} \tag{9a}$$

$$r'(\pi/3) = 47{,}400 \text{ psi} \tag{9b}$$

$$r'(2\pi/3) = 42{,}500 \text{ psi} \tag{9c}$$

$$r'(\pi) = 34{,}500 \text{ psi} \tag{9d}$$

Two additional conditions are possible if the π-plane curve is not to have an abrupt change in slope as it crosses the axis of symmetry. These are

$$\frac{dr'(\theta)_o}{d\theta} = 0 \tag{10a}$$

$$\frac{dr'(\theta)_\pi}{d\theta} = 0 \tag{10b}$$

Since six restraints are put on $r'(\theta)$, we can write

$$r'(\theta) = a + b\theta + c\theta^2 + d\theta^3 + e\theta^4 + f\theta^5 \qquad (11)$$

and easily obtain the values for the coefficients. By inspection, condition (9a) gives a = 49,500 psi and condition (10a) gives b = 0. The remaining four conditions are used to develop the following system of equations:

$$(\pi^2/9)c + (\pi^3/27)d + (\pi^4/81)e + (\pi^5/243)f = -2100 \qquad (12)$$

$$4(\pi^2/9)c+8(\pi^3/27)d+16(\pi^4/81)e+32(\pi^5/243)f = -7000 \qquad (13)$$

$$\pi^2 c + \pi^3 d + \pi^4 e + \pi^5 f = -15000 \qquad (14)$$

$$2\pi c + 3\pi^2 d + 4\pi^3 e + 5\pi^4 f = 0 \qquad (15)$$

These equations, upon simultaneous solution, give c = 5651.64, d = 6210.6, e = 3005.64 and f = 460.72, thus

$$r'(\theta) = [49500-5651.64\theta^2 + 6210.6\theta^3 - 3005.64\theta^4 + 460.72\theta^5] \text{ psi} \qquad (16)$$

It is customary to reference angles in the π-plane to line $\overline{OP}$ in figure 31 and in this case

$$\theta = (\theta' - \pi/6) \qquad (17)$$

where

$$\theta' = \text{TAN}^{-1} \frac{1}{\sqrt{3}} \frac{2\sigma_3 - \sigma_2 - \sigma_1}{\sigma_2 - \sigma_1} \tag{18}$$

Equation (18) and its development can be found in most plasticity textbooks. Once again, by invoking the assumption of symmetry with respect to the axis of prestraining it is clear that we must use the magnitude of the quantity $(\theta'-\pi/6)$ so that a negative θ will see the same yield criterion as a positive θ of the same value. Hence, equation (17) becomes

$$\theta = |\theta'-\pi/6| \tag{19}$$

The sequential application of equations (18), (19) and (16) represents the application of the subsequent yield criteria for 304 stainless steel prestrained as described herein. As long as the effective stress level which has a direction coinciding with a given θ does not exceed the value predicted for that θ then yielding has not occurred.

In the preceding discussions, the methods used to represent the empirical subsequent yield data for 304 stainless steel have been put forth without regard for the shape of the yield locus between the points in the deviatoric plane which have been determined. Nevertheless, the use of these mathematical representations will result in an improvement in accuracy over the use of more common

subsequent yield theories such as those of von Mises and Prager. Since the six empirical data points in the deviatoric plane can be represented, with varying degrees of accuracy, by a great number of curves, some thought must be given to determining the shape of the subsequent yield locus in the sections lying between the data points. Several possibilities exist for investigating the yield locus in these sectors.

One experimental approach might involve the use of hollow thin-walled cylinders subjected to combined internal pressure and axial tension while submerged in a pressure environment. Such cylinders could easily be machined from prestrained parent specimens of the type used in this project. By carefully controlling the increase in the axial load and internal pressure applied to the specimen, states of biaxial tensile stress can be developed which will permit the subsequent yield locus to be examined at points in the deviatoric plane other than those lying on the tensile or compressive segments of the principal axes. These tests could be conducted at various pressure environments simply by changing, by an equal amount, both the pressure inside the cylindrical specimen and the pressure surrounding the specimen.

Although the technique of using thin-walled cylinders would be a valuable compliment to the techniques used in this project, it is still not the ultimate solution to the problem of experimentally defining a subsequent yield surface.

Since the longitudinal axis of the cylindrical specimen would be colinear with the longitudinal axis of the parent specimen from which the cylinder was cut, biaxial tensile states of stress could only be developed on pairs of axis which included the axis of prestrain. This leaves a significant portion of the subsequent yield surface beyond the reach of this experimental technique. In addition to this drawback, the technique would require specimen support and loading hardware of substantially greater complexity than was required for the tests reported here.

A sub-specimen that develops a state of pure shear could also be used to better define the subsequent yield surface in the regions between the extended principal axes of prestrain. The stress states that result from this type of test consist of two principal stresses which are equal in magnitude but opposite in sign and a third principle stress which is zero. Thus, it is possible to intersect the yield surface with stress probes having projections in the deviatoric plane that bisect the vertex angle of the 60° sectors under consideration. The problem of generating the required stress states in the sub-specimens is, however, great. Torsional loading of hollow cylinders is undesirable because of the principal stress axes rotation discussed earlier. A better choice might be the use of notched strip sub-specimens. Such specimens require only simple apparatus since the test procedure involves a tension test of a thin notched strip of rectangular cross-section. Although this technique has been

discussed in some detail by Biljaard[17] and Hill[18], additional refinements could be made through the use of finite element stress analysis programs. Because the notched strip specimens need only be loaded in tension, running the tests in variable fluid pressure environments would not present any particularly complex procedural problems.

Finally, it may be possible to approximate the shape of the yield locus between the known experimental points in the deviatoric plane by using available experimental data pertaining to the nature of the stress-incremental strain relations for plastic flow. Equation (18) can be written as

$$\text{TAN } \theta' = \frac{1}{\sqrt{3}} \mu \tag{20}$$

where μ is the Lode stress parameter, or

$$\mu = \frac{2\sigma_3 - \sigma_2 - \sigma_1}{\sigma_2 - \sigma_1} \tag{21}$$

Similarly, in terms of the plastic strain increment components, we can write the strain parameter ν as

$$\nu = \frac{2d\varepsilon_3^p - d\varepsilon_1^p - d\varepsilon_2^p}{d\varepsilon_2^p - d\varepsilon_1^p} \tag{22}$$

and

$$\text{TAN}\Psi = \frac{1}{\sqrt{3}}\nu \tag{23}$$

where Ψ is equivalent to θ' in principal strain space. If the principal plastic strain increment axes are superposed on the principal stress axes it is easy to see that assumed coaxiality of the stress vector and the plastic strain increment vector implies that $\theta' = \Psi$, or

$$\mu = \nu \tag{24}$$

Equation (24) is a manifestation of the Prandtl-Reuss flow law. Deviations from this flow law have shown up in the experiments of Lode[19] and Taylor and Quinney[20]. The results of these experiments are shown, respectively, in figures 32 and 33. The case of $\mu = 0$ represents a state of pure shear while $\mu = \pm 1$ represents uniaxial stress.

Consider, now, the construction shown in figure 34. Arc $\overline{AC}$ represents a yield locus in the deviatoric plane and θ' is referenced to line $\overline{OP}$ as in figure 31. The vector $\overline{BD}$ represents the projection of the plastic strain increment vector and is drawn colinear with the outward normal to the yield locus at B to be compatible with the assumption that the yield criterion serves also as a plastic potential, $g\ (\sigma_{ij})$, from which the ratios of the

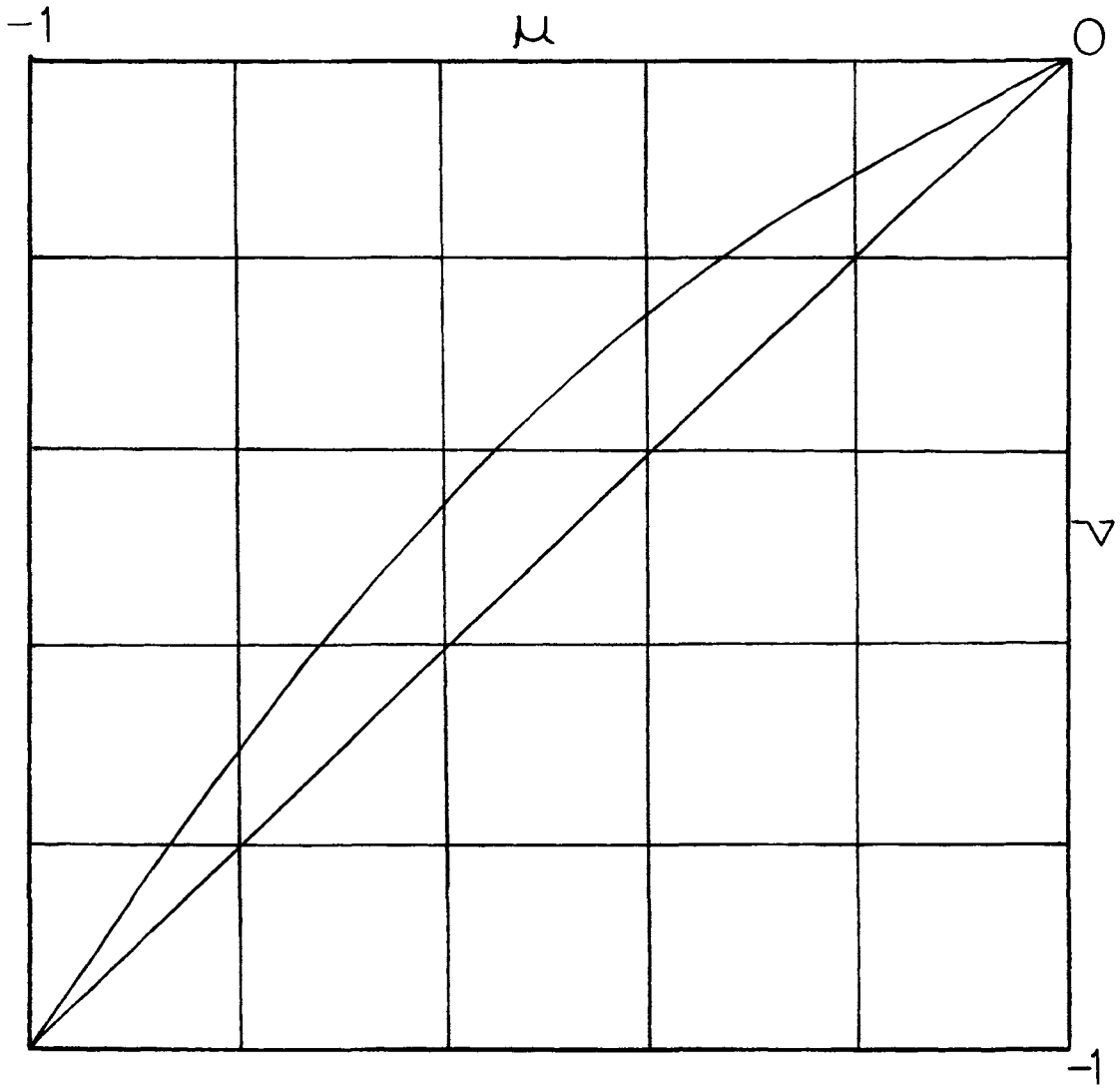

Figure 32 - Results of Lode

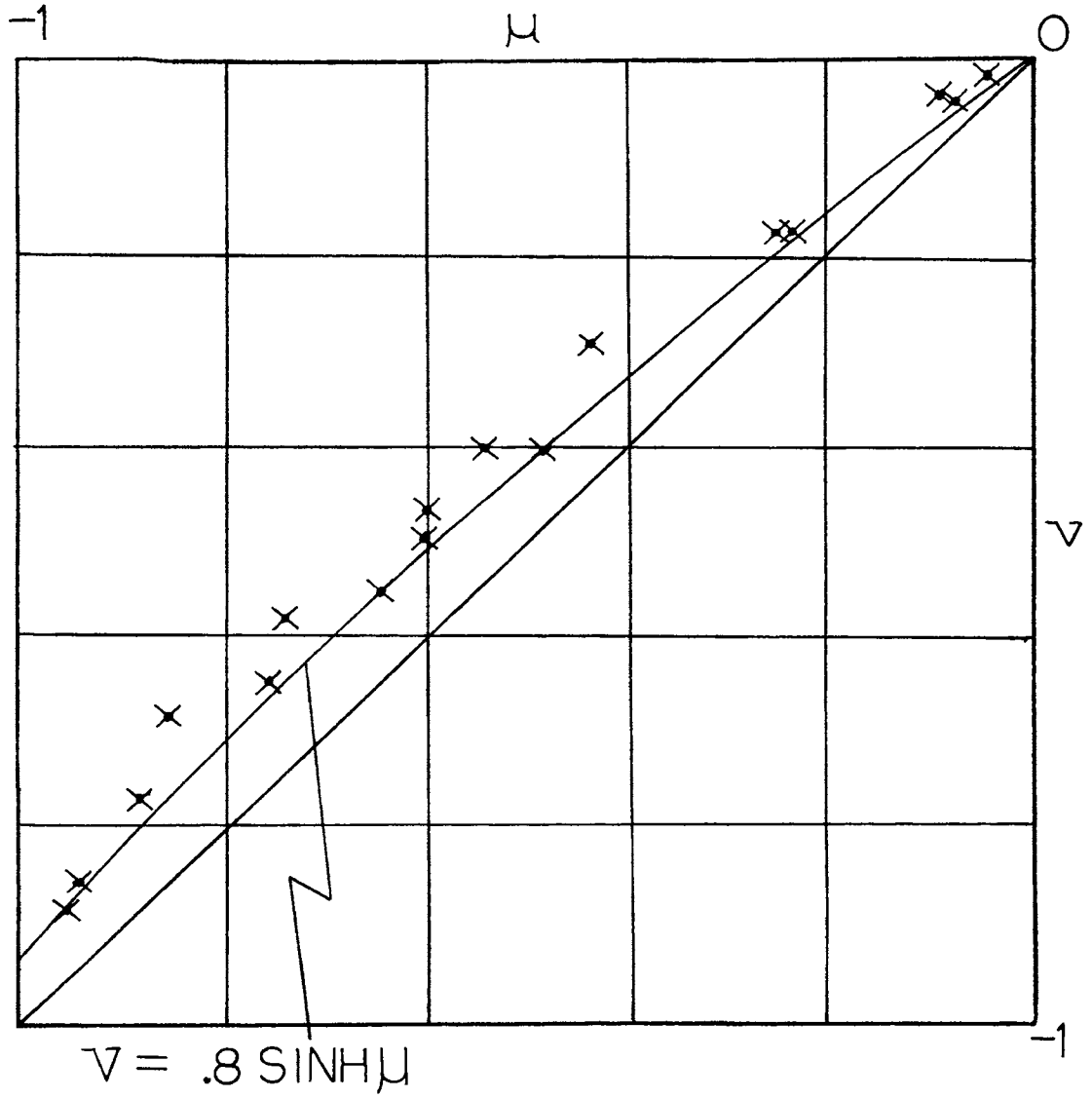

Figure 33 - Results of Taylor and Quinney

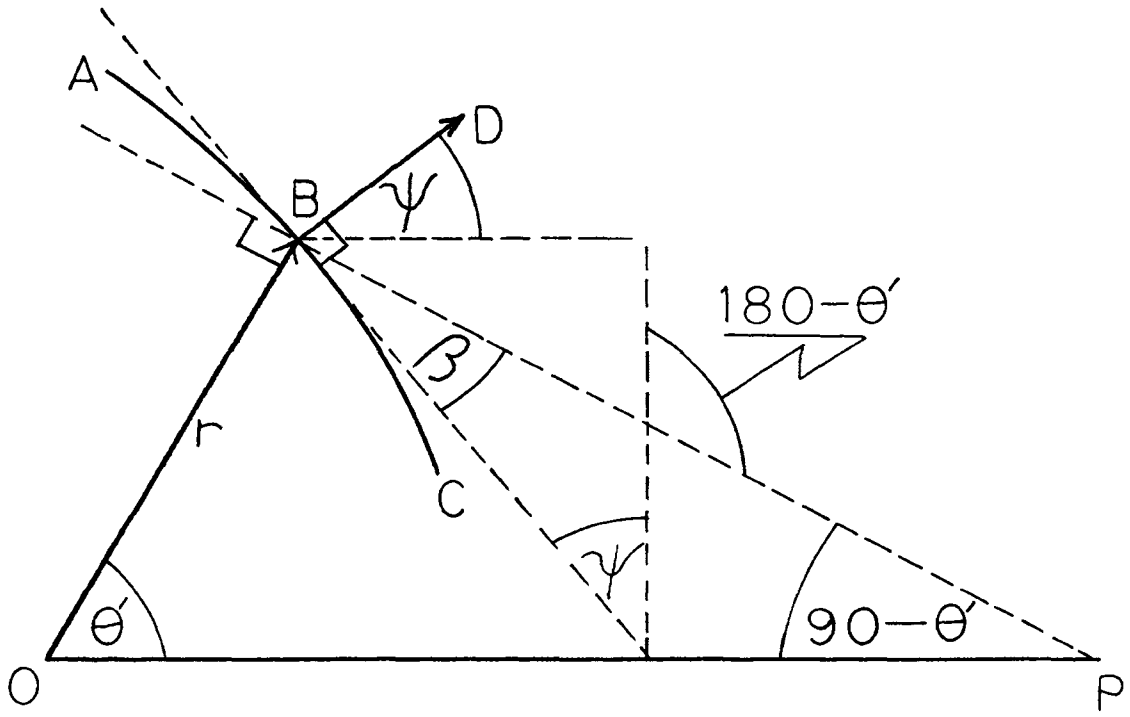

Figure 34 - Plastic Strain Increment Vector in Relation to the Yield Surface

components of the plastic strain increments are derivable by partially differentiating $g(\sigma_{ij})$, with respect to σ_{ij}. The colinearity of the outward drawn normal at B and the vector BD follows because the direction cosines of the outward drawn normal to the yield surface $g(\sigma_{ij})$ at $(\sigma_1, \sigma_2, \sigma_3)$ are, from three-dimensional Cartesian geometry,

$$\frac{\partial g}{\partial \sigma_1}, \quad \frac{\partial g}{\partial \sigma_2}, \quad \text{and} \quad \frac{\partial g}{\partial \sigma_3} \tag{25}$$

Thus, we see from figure 34, that

$$\Psi + (180 - \theta') + \beta = 180° \tag{26}$$

or

$$\beta = \theta' - \Psi \tag{27}$$

Therefore,

$$\frac{dr}{r d\theta'} = \text{TAN}\beta = \text{TAN}(\theta' - \Psi) \tag{28}$$

or

$$r = r_o \exp\left(\int_o^{\theta'} \text{TAN}(\theta' - \Psi)\, d\theta' \right) \tag{29}$$

Since the relation between μ and ν can be estimated by considering figures 32 and 33, equation (29) can be

evaluated. Choosing

$$\nu = .8\ \mathrm{SINH}(\mu) \tag{30}$$

gives, with equations (20) and (23),

$$\mathrm{TAN}(\theta' - \Psi) = \frac{\left[\mathrm{TAN}\theta' - \left(\frac{.8\ \mathrm{SINH}\ (\sqrt{3}\ \mathrm{TAN}\theta')}{\sqrt{3}}\right)\right]}{\left[1 + \mathrm{TAN}\theta'\left(\frac{.8\ \mathrm{SINH}\ (\sqrt{3}\ \mathrm{TAN}\theta')}{\sqrt{3}}\right)\right]} \tag{31}$$

Equation (31) permits equation (29) to be evaluated. The yield locus thus obtained for the sector lying between the line $\overline{OP}$ and the negative σ_1 axis in figure 31 is shown, with the polynomial-fit curve, in figure 35. For this display the radius r_o in equation (29) was taken as the radius $\overline{OP}$ in figure 31. Under other circumstances, r_o might be evaluated from, say, a pure shear test as described earlier. The use of equation (29) is somewhat limited, however, since it is a μ-ν relationship that cannot necessarily be extended or extrapolated to all sectors of the deviatoric plane. It is usually assumed that only values of μ varying from +1 to -1 need be considered due to the similarity of each of the 60° sectors in the deviatoric plane formed by the extended principal stress axes. However, the degree of isotropy required for the similarity of these sectors is not present in the prestrained 304

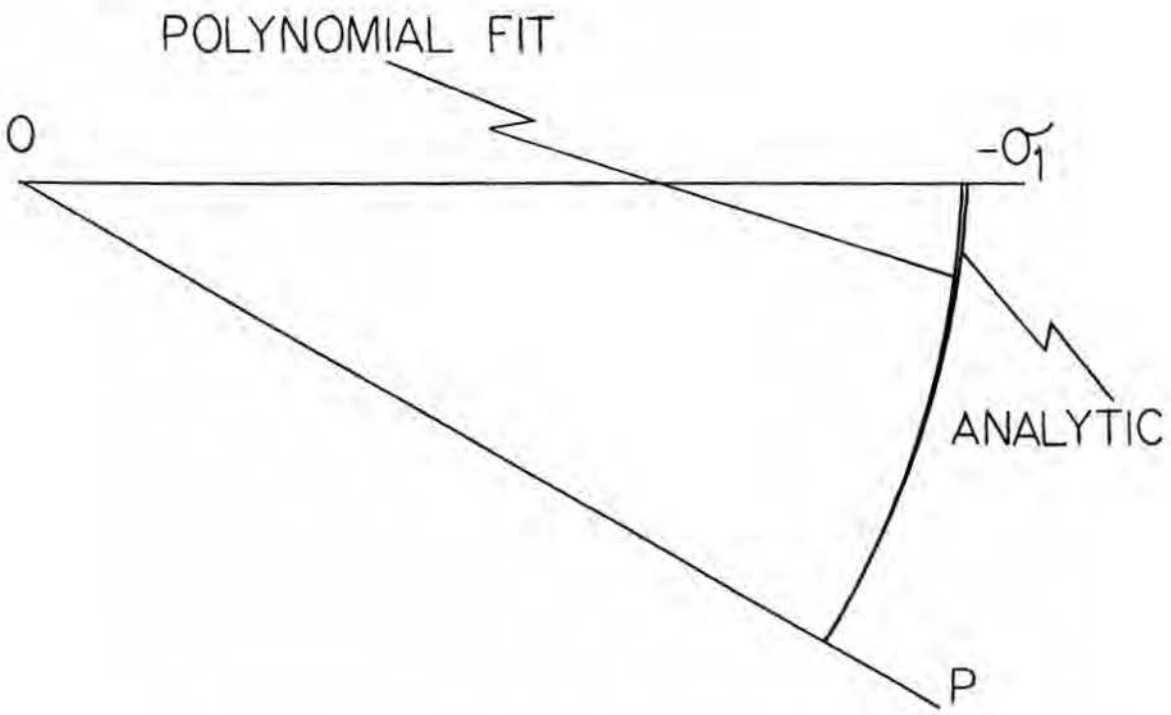

Figure 35 - Analytic Approximation of Yield Surface Compared to Polynomial Fit Section

stainless steel tested here. This technique holds promise for the future when more is known about the flow laws which govern radically isotropic plastic flow.

V. CONCLUSIONS

The shape of the subsequent yield surface for 304 stainless steel for a particular degree of prestrain has been found to differ with the predictions of the subsequent yield theories currently in existence. Although the empirically determined yield surface does not conform to the predictions of any particular subsequent yield theory, the surface can be thought of as a hybrid which embodies the features of both the von Mises isotropic hardening theory and the Prager kinematic hardening theory. This hybrid characteristic permits the subsequent yield criteria to be expressed mathematically in a manner similar to the von Mises virgin yield criteria. In addition, conventional polynomial curve fitting methods can be used to more accurately describe the subsequent yield locus in the deviatoric plane.

The experimental techniques used in this project allowed the determination of six points on the deviatoric subsequent yield locus. This is a bare minimum and other tests for the prestrained sub-specimens should be developed to supplement the work done here. Two possibilities are the use of thin-walled cylindrical specimens, loaded by axial tension and internal pressure, and notched strip tensile specimens.

The author proposes, also, that subsequent yield criteria for more complex types of prestraining can be similarly developed. For the material used in this project, the only information required to promulgate an approximate

subsequent yield criteria is the direction of the pre-stressing as seen in the π-plane and the increase in effective stress achieved at yield in this direction. It should not be necessary to prestrain along a principal axis to obtain results as shown in the previous section. It must be noted, however, that this is speculative and additional work is needed for verification.

It is also desirable to extend the methods and techniques of this project to other materials and, particularly, to other degrees of prestrain for the 304 stainless steel alloy. Since the mechanism for plastic flow is similar for all of the austenitic stainless steels, it is expected that they behave in a manner much like the 304 alloy did in these tests. The ferretic and martensitic stainless steel alloys may differ substantially from the performance of 304 stainless under these conditions. Beyond stainless steels, there exists a myriad of other materials yet to be examined for their subsequent yield behavior. Although Hu's work on Nittany No. 2 Brass is based on only fragmentary data, it does show with this paper, that more than one possibility exists for a subsequent yield surface shape. Little more can be said about the nature of the subsequent yield phenomena without additional experimental work.

In the case of 304 stainless steel, the subsequent yield surface was such that the shape of its intersection

with planes normal to the hydrostatic axis did not change with the position of each normal plane along the hydrostatic axis. This feature made it relatively easy to represent the subsequent yield surface mathematically. In cases like this, or even in cases where the pressure effect on yield is apparent, subsequent yield criteria can be developed which are not difficult to apply - no more difficult, in fact, than those of Tresca and von Mises.

VI. BIBLIOGRAPHY

1. Dieter, G., Mechanical Metallurgy, McGraw-Hill, New York, 1961, p. 150.

2. Bridgman, P. W., Studies in Large Plastic Flow and Fracture, Harvard University Press, Cambridge, 1964, p. 317.

3. Prager, W., "The Theory of Plasticity," Proceedings of the Institution of Mechanical Engineers, London, 1955, pp. 3-19.

4. Naghdi, P. M., Essenberg, F., and Koff, W., "An Experimental Study of Initial and Subsequent Yield Surfaces in Plasticity," Journal of Applied Mechanics, vol. 25, 1958, pp. 201-209.

5. Ivey, H. J., "Plastic Stress-Strain Relations and Yield Surfaces for Aluminum Alloys," Journal of Mechanical Engineering Science, vol. 3, 1961, pp. 15-31.

6. Smith, S., and Almroth, B. O., "An Experimental Investigation of Plastic Flow under Biaxial Stresses," Experimental Mechanics, vol. 10, no. 6, 1970, pp. 217-224.

7. Mair, W. M., and Pugh, H. Ll. D., "The Effects of Pre-Strain on Yield Surfaces in Copper," Journal of Mechanical Engineering Science, vol. 6, 1964, pp. 150-163.

8. Iagn, Iu. I., and Shishmarev, O. A., "Some Results of an Investigation of Elastic State Limit of Plastically Drawn Nickle Samples," Doklady Akadamii Nauk, USSR, vol. 119, 1958, pp. 431-433.

9. Hsu, T. C., "The Effect of the Rotation of the Stress Axes on the Yield Criterion of Prestrained Materials," Journal of Basic Engineering, Mar. 1966, pp. 61-70.

10. Hu, L. W., and Bratt, J. F., "Effect of Tensile Plastic Deformation on Yield Condition," Journal of Applied Mechanics, vol. 25, Trans. ASME, vol. 80, 1958, p. 411.

11. Hu, L. W., Shull, H. E., and Pae, K. D., "Effect of Tensile Plastic Deformation on Three Dimensional Yield Surfaces," AFOSR Report 1716, 1961, pp. 36-62.

12. Prager, W., "Models of Plastic Behavior," Proceedings of the Fifth U. S. Congress on Applied Mechanics, ASME, 1966. pp. 435-450.

13. Gordon, R. B., and Tien, J. K., "Use of Electrical Resistance Strain Gages under Hydrostatic Pressure, ASME

publication 64-WA/PT-20.

14. Gerdeen, J. C., "Effects of Pressure on Small Foil Gages," Proceedings of the SESA, vol. XX, no. 1, pp. 73-80.

15. Milligan, R. V., "Effects of High Pressure on Foil Strain Gages," Experimental Mechanics, vol. 4, pp. 25-36.

16. Pugh, H. Ll. D., personal communication, 1970.

17. Biljaard, P. P., Publication of the International Association of Bridge and Structural Engineering, vol. 6, no. 27.

18. Hill, R., The Mathematical Theory of Plasticity, Oxford, University Press, 1950, Ch. 12.

19. Lode, W., "Versuche uber den Einfluss der mittleren Hauptspannung auf das Fliessen der Metalle Eisen, Kupfer und Nickel," Zeitsch. Phys., vol. 36, p. 913.

20. Taylor, G. I., and Quinney, H., "The Plastic Distortion of Metals," Philosophical Transactions of the Royal Society, Series A, vol. 230, p. 323.

VII. VITA

Joseph George Hoeg was born on December 13, 1943, in Wilkes-Barre, Pennsylvania. He received his primary and secondary education in Dallas, Pennsylvania, and was awarded a Bachelor of Science Degree in Mechanical Engineering by the University of Maryland in June, 1965. Upon completion of his undergraduate work, he accepted a position in the United States Department of the Navy and currently serves that organization in the capacity of a Structures and Materials Consultant.

He has been enrolled in the Graduate School of the University of Missouri-Rolla since September, 1966, and was awarded a Master of Science Degree in Engineering Mechanics in June, 1968. Subsequent to this, the author held a National Science Foundation Fellowship at the University of Missouri-Rolla while pursuing the degree Doctor of Philosophy.